Finite Element based Redesign and Optimization of Aircraft Structural Components using Composite Materials

Sergio Andrés Ardila-Parra, Carmine Maria Pappalardo, Octavio Andrés González Estrada, Domenico Guida

Finite Element based Redesign and Optimization of Aircraft Structural Components using Composite Materials

Sergio Andrés Ardila-Parra, Carmine Maria Pappalardo, Octavio Andrés González Estrada, Domenico Guida

***Abstract*—In the preliminary stage of the industrial design, the structural analysis of the components made of composite materials is generally difficult to carry out for aircraft structures having complex three-dimensional geometry. More importantly, in the case of composite structures, the lay-up process creates a particular distribution of the material properties that is challenging to simulate in a virtual environment. This research work is, therefore, focused on the use of the finite element method for the numerical analysis and the structural redesign of the bulkhead and flap aircraft components. In particular, the numerical results obtained in this work are the stress and strain fields of these mechanical components. The redesign and the structural optimization of these two mechanical components are performed employing a simple numerical procedure. For this purpose, the quality of the stress and strain fields obtained by performing numerical experiments is evaluated considering failure criteria suitable for composite structures. Subsequently, the analysis developed in this study is used for determining the performance of the material as well as the number and orientation of the plies selected for the composite components. The verification process performed in this work, on the other hand, consisted of a comparative analysis with the same aerospace components made of isotropic and anisotropic materials. The numerical results found are compared with the experimental results available for the aerospace components that are geometrically and functionally similar to the bulkhead. In general, a good agreement is found in the comparison between the numerical and experimental results.**

***Index Terms*—Finite element method, Design optimization, Component redesign, Structural analysis, Composite materials.**

I. Introduction

The principal goal of this paper is to develop three-dimensional mechanical models of the main structural components of a general-aviation single-engine aircraft. The mechanical models constructed in this research work will serve as the basis for the system parameter identification and the structural health monitoring of aircraft components that will be performed in future investigations [1]–[5]. Background information, the formulation of the problem of interest for this investigation, a short literature review, the scope and the contributions of this study, and the organization of the manuscript are provided in this introductive section.

S. A. Ardila-Parra is with the *School of Mechanical Engineering, Universidad Industrial de Santander*, Calle 27, 9, 680002 Bucaramanga, COLOMBIA (email: sergio.ardila.parra@outlook.com).

C. M. Pappalardo is with the *Department of Industrial Engineering, University of Salerno*, Via Giovanni Paolo II, 132, 84084 Fisciano, Salerno, ITALY (corresponding author, email: cpappalardo@unisa.it).

O. A. González Estrada is with the *School of Mechanical Engineering, Universidad Industrial de Santander*, Calle 27, 9, 680002 Bucaramanga, COLOMBIA (email: agonzale@uis.edu.co).

D. Guida is with the *Department of Industrial Engineering, University of Salerno*, Via Giovanni Paolo II, 132, 84084 Fisciano, Salerno, ITALY (email: guida@unisa.it).

A. Background Information

In modern engineering design and manufacturing, the use of computer-aided modeling and the performance assessment by means of numerical simulation has conquered a central role. Since computer simulations are becoming more and more effective and efficient, well-defined computer models allow for developing faster and cheaper processes for the design cycle. However, it is apparent that the reliability of the numerical results obtained employing computer simulations depends on their accuracy, evaluated in comparison with the experimental measurements obtained operating on the actual physical system [6], [7]. It is, therefore, of paramount importance for the engineer to develop appropriate computer models of the physical system to be analyzed in order to be able to construct a viable design.

Nowadays, commercial as well as free computational finite element software have advanced capabilities based on sound theoretical formulations. Once a computer model of a physical system has been developed, the computational tools embedded in the computer-aided software derive the mathematical models which describe the physics of interest for the system to be analyzed. However, the experience of the engineer still plays a fundamental role in the preliminary mechanical design phase, in the correct interpretation of the numerical results obtained by using computational tools, and in the iterative redesign process of a given structural component [8], [9]. For instance, the tools of pre and post-processing allow for assessing the quality of the desired design solution and the subsequent detailed development and optimization of the mechanical structure previously modeled in a virtual environment [10], [11]. Also, these numerical packages allow us for solving multiphysics problems, can be used for performing the fatigue analysis, and provide an estimation of the damage tolerance of a mechanical part. Thus, the numerical solutions obtained in a virtual environment by means of the mathematical models developed by the engineer needs to be refined and interpreted, thereby allowing for verification with the actual physical system of interest.

The increasing complexity of the structural components employed in modern engineering applications needs powerful computational tools for analysis [12]. To this end, the most used approaches are the Finite Element Method (FEM) and the Boundary Elements Method (BEM) [13], [14]. Both the FEM and the BEM represent effective computational

approaches for obtaining a numerical solution of a given structural problem described by Partial Differential Equations (PDEs). In the FEM, the spatial domain of a structural system to be analyzed is divided into small portions connected to each other called finite elements [15], [16]. Within the spatial sub-domain of a single finite element, the solution of the underlying partial differential solution is approximated with an interpolating solution based on the value of the solution computed at the finite element nodes. The local approximate solutions can be subsequently assembled to yield a global approximate solution. For elasticity problems, the FEM is the numerical counterpart of the analytical solution which can be obtained, at least in principle, by using the Rayleigh-Ritz method. In the BEM, on the other hand, the spatial discretization is performed only on the boundary of the continuous system to be analyzed [17]. The fact that, in the BEM, the discretization process is carried out only on the system boundary represents the main difference between this method and the FEM in which the spatial domain of the system of interest is completely discretized. Basically, the BEM is obtained from the discretization of an integral equation mathematically equivalent to the original problem. Subsequently, one can recover an approximate solution at points inside the spatial domain from the numerical solution obtained by using the BEM on the boundary of the system of interest. Since in practical engineering applications, which involve complex three-dimensional geometry, the BEM has several limitations when compared with the FEM, the FEM is used in this investigation for the structural redesign and optimization of aircraft components.

The computational strategy based on the finite element approach is particularly suitable for evaluating the static deformation of the aircraft fuselage in response to the externally applied loads. In particular, the numerical analysis based on the FEM is greatly useful when the three-dimensional geometry of the mechanical component of interest has a complex shape. From a computational point of view, the analytical formulation of static problems solved by using the FEM is based on converting a complex mathematical problem formulated in terms of Partial Differential Equations (PDEs) into a simpler mathematical problem formulated in terms of Ordinary Differential Equations (ODEs) which approximate the original problem and can be conveniently formulated in a compact matrix form [18]. This computational approach provides an approximate solution for a finite number of nodal points called finite element nodes. The numerical solution for the remaining part of the spatial domain can be readily obtained by means of an interpolation process using the numerical solution found for the nodal coordinates. Therefore, the final numerical solution represents only an approximate solution in which the discretization error is averaged throughout the spatial domain. The material points where the numerical solution is found are called joint nodes and this set of nodes forms a network called finite element mesh. The portions of the spatial domain that form the union of the material nodes of the mesh are called finite elements. In aerospace applications, the deformation field to which the aircraft fuselage is subjected can be obtained employing the FEM and, with the use of these numerical results, the strain and stress fields can be calculated in order to evaluate the critical points of the mechanical design. Another important aspect is the point that the predictions obtained by means of a finite element numerical procedure require an experimental validation for increasing the confidence in the numerical results and for evaluating the practical feasibility of the design. Furthermore, the numerical analysis obtained through the FEM represents a valid alternative applicable in conjunction with the analytical results derived using theoretical methods and can be implemented for complicated components for which the analytical solution is extremely difficult to obtain. Since the theoretical calculations of the structural performance of aircraft components made with composite materials are even more difficult, if not impossible, to obtain with respect to other materials, the FEM can be a useful and reliable substitute in the resolution of these complex problems where the theory can only guide the intuition of the analyst [19].

B. Formulation of the Problem of Interest for this Investigation

In the aerospace industry, the use of composite materials in the construction of aircraft components has increased up to half of the total weight [20]. In particular, the use of Fiber-Reinforced Polymer Composites (FRPs) has been widely implemented in aerospace engineering for reinforcing several types of matrices like polymeric or the ceramic matrices. Some of the most important characteristics that make these materials so popular are their low weight since they are lighter than metals, their great resistance, and their good fatigue performance. FRPs also possess high fracture toughness, high damage tolerance, and there are several design and manufacturing techniques available that are economically affordable and easy to implement. Furthermore, in general, the use of composite materials requires fewer joints and rivets in the construction of mechanical components which induces greater reliability to the aircraft composite parts [21].

In the design of aircraft components and in many other modern industrial applications such as the automotive industry, it is important to carry out the structural analysis of the mechanical parts before their construction and implementation. The structural analysis allows for reducing the manufacturing and prototyping costs. Furthermore, in the aerospace industry, this type of analysis allows for improving the efficiency of light mechanical components and, therefore, leads to a reduction of the fuel consumption of the aircraft. Employing appropriate computational approaches, such as the finite element method, it is possible to adequately simulate the stresses and strains that occur in the fundamental mechanical components of aircraft, such as the flaps of the aircraft. By doing so, one can identify the critical points in the geometric design of these fundamental components and improve the performance of material selected for manufacturing these mechanical parts.

In several modern aerospace applications, one of the main goals is to perform the redesign of the bulkhead and the flaps using composites materials for their manufacture. For example, after the development of fiber epoxy laminates, these materials have been readily implemented in several components of the aircraft such as the wing structures, the fuselage, and the ballistic protections [22]. The principal advantages associated with the use of composite materials

are the significant weight reduction, the high strength and stiffness, the good fatigue properties, and great corrosion resistance. However, the construction of appropriate numerical models of these fundamental components, which are developed by means of a computer-aided design and engineering process that allows for assessing the behavior of these mechanical parts before and after the redesign with composite materials, still represents a challenging task. This interesting problem represents the principal issue addressed in this investigation. In particular, the main reason behind the use of composite materials, such as fiber carbon fabrics, is the reduction of the total weight of the aircraft. By doing so, it is possible to achieve a reduction in the fuel consumption of the aircraft. As discussed in detail in the paper, composite materials are widely used in aeronautical applications and are replacing traditional materials such as aluminum alloy.

C. Literature Review

In recent years, several studies on the structural analysis of composite materials have been developed, thus demonstrating the importance of this topic for engineering applications [23], [24]. Computational tools have been introduced in aerospace engineering to enhance component characteristics such as the geometric shape, the material, and the manufacturing process, as well as the total cost and the environmental impact [25]. In aerospace engineering, numerical methods such as the FEM and BEM have been used in the structural analysis of the aircraft fuselages. Soutis achieved the optimization of the design of a fuselage by calculating the orientation of the fibers as well as the sequence of stacking of the laminate [26]. Buehrle et al. used a finite element approach to predict the structural dynamics of robust aircraft models analyzing the behavior of structures with different stiffness [27]. Mukhopadhyay analyzed the structural performance of fuselages having complex geometries, generally not circular, comparing the skin of the fuselages made with sandwich and panels of composite materials, thereby achieving the most viable type of skin in terms of resistance and manufacturing costs, and one of the fuselage components most studied and analyzed using FEM was the bolted joint [28]. Calado et al. developed a computational tool based on the finite element approach to supports the designer in the selection of the most suitable configuration for the carbon fiber-reinforced composite for aircraft structures (orientations, the number of plies, material type, etcetera) [29]. Kassapoglou compared different manufacturing process to optimize the design of fuselage frames considering minimum weight, minimum cost, or a combination of the two [30], [31]. Thoppul et al. proposed a methodology to predict the behavior of the material due to the concentrated efforts in the holes that make the union possible [32]. Kaye and Heller performed the shape optimization of a metallic airframe for the FS470 bulkhead to extend its fatigue life [33]. Marusich et al. developed a finite element model to specifically predict distortions due to the application of machining-induced stresses over commercial and military aircraft [34]. Germaneau et al. studied the displacements in plain bearings that are used to joint fuselage and wings while the results were verified with a finite element model [35]. Guida and Marulo, Fasanella et al., and Kumajura assessed the fuselage structural performance under abrupt loads like those that occur in a crash due to an emergency landing [36]–[39].

In the literature, the structural analysis of mechanical systems has been used in the redesign and optimization of several components of the aircraft such as the fuselages or the wings [40]. This type of analysis is aimed at reducing the weight of the system components or improve the aerodynamic behavior of the aircraft [41]. Hansen et al. investigated the design of integrated aircraft systems in which the wings and the fuselage form a single structural element [42]. Ivanov developed a finite element model using two-dimensional beam elements in order to optimize the layer thicknesses of composite laminated components [43]. Esnaola et al. used the finite element analysis and experimental tests for predicting the crushing behavior of semi-hexagonal E-glass/polyester composite structures [44]. Sliseris et al. developed optimization procedures to obtain the optimum design for glass fiber reinforced polymer plywood plates and a finite element analysis was used to evaluate the quality of the final results [45]. Several research studies are focused on optimization algorithms to improve the design in terms of the production cost, see for example the work of Mukhopadhyay et al. [46]. In the study of Witik et al. [47], alternative methods to produce aircraft composite components were analyzed, while Van den Kieboom and Elham focused on the minimization of the fuel consumption [48]. Dillinger et al. demonstrated a viable solution for the stiffness optimization of composite wings [49]. Non-circular fuselage shapes have also been studied, like in the work of Thomsen and Vinson that studied the sandwich theory to analyze this structure [50], and Liu et al. which optimized a lattice composite fuselage structure [51]. However, most studies focus only on the fuselage and/or on the wing skin. Consequently, it is necessary to expand the studies on the analysis of other components that serve as structural parts of an aircraft. Very few researches are focused on the structural components of the aircraft such as the ribs, the bulkhead, the cabins, or the flaps [52]–[55]. This issue is addressed in the present research work.

The major challenge faced by the researchers in structural optimization is to develop methods that are suitable for use with the complex general-purpose software package available for structural analysis [56], [57]. This problem is particularly challenging in the case of the aerodynamic design. In fact, the aerodynamic design affects all aspects of the structural design, while the structural design affects the aerodynamic design primarily through a single number-the structural weight. This asymmetry in the mutual influence of aerodynamic and structural designs means that the problem can be treated as a two-level optimization problem, with the aerodynamic design at the upper level and the structural design at the lower level [58]. The problem of finite element generation in shape optimization is due to the fact that in most cases the definition of a finite element mesh is a manual rather than an automated process. That is, the analyst uses judgment and experience-based intuition to select the mesh [59]. In view of the increasing use of optimization methods for structural analysis, there is merit in considering again the simultaneous approach to analysis and design. Furthermore, when optimization techniques are used for structural analysis, the design problem becomes a nested optimization problem.

One way of adding optimization capabilities to a finite element program is to add a simple resizing scheme based on the fully stressed design approach or a more rigorous optimality criterion. For plate elements with in-plane loads and subject to only stress constraints, the stress-ratio technique has been very popular [60].

Over the past few decades, increasingly powerful high-performance computational resources and the development of sophisticated numerical algorithms have enabled the solution of large-scale, high-fidelity structural design optimization problems [61]. Since structural weight reduction is critical in many aerospace applications, the most common structural design problem is to minimize the structural mass subject to stress and possibly buckling constraints. These structural constraints are imposed at a series of design load cases to ensure the safety of the aerospace vehicle within a prescribed operational envelope [62]. Design optimization is a numerical tool used in many engineering design applications to find the optimal solution to a given design problem. The use of optimization is of particular importance in aircraft design, where there is a continuous demand to improve performance [63]. The continued growth of air traffic has caused increasing demands to reduce aircraft emissions, imposing new constraints on the design and development of future airplane concepts. Moreover, during the past decades, the advancement of numerical methods for the analysis of complex engineering problems, such as those found in fluid dynamics and structural mechanics, has reached a mature stage: many difficult numerically intensive problems are now readily solved with modern computer facilities [64], [65]. The present research paper is collocated in this context and tries to contribute with a simple and effective optimization procedure applicable to the redesign of the fundamental aircraft components.

D. Scope and Contributions of this Study

This work deals with the redesign and the optimization of the flap and of the bulkhead of a general aviation single-engine aircraft which represent fundamental structural components. In particular, one of the main objectives of this work is to investigate the performance of the redesign of these structural components based on composite materials. From a general perspective, the structural analysis of mechanical components made of composite materials represents a challenging engineering problem, especially for aircraft structures featuring complex three-dimensional geometry. In order to solve this structural engineering problem, there are several important issues to address. To this end, finite element models of the mechanical components of interest for this study are developed starting from detailed three-dimensional CAD models. The numerical results found in the finite element analysis performed in this investigation are the stress and strain fields of the mechanical components. Furthermore, the vertical displacements of the critical points of these structural components induced by the loading conditions are compared with the experimental data available. A simple optimization strategy is used in this investigation for the structural redesign of the aircraft components considered in this study.

In this paper, a thorough numerical analysis is carried out in order to verify the effectiveness of the redesign of two important aeronautical components of a general-aviation single-engine aircraft. In particular, the mechanical components considered in this work are the bulkhead and the flap of the aircraft. While the bulkhead is a structural component of the fuselage, the flaps are important mechanical parts of the wings. In order to address and solve the structural redesign and optimization problems of interest in this study, there are several important issues to take into account. For instance, the correct representation of the mechanical properties of computational models by means of an adequate selection of the direction of the fibers of the composite components, the use of an appropriate meshing strategy for constructing a finite element model of the mechanical components, the determination of a consistent set of boundary conditions necessary for performing the static analysis, the use of a proper solution approach based on a robust and reliable computational tools arising from a sound analytical approach, and the experimental verification of the methodology implemented are, among the others, important examples of the fundamental issues considered in this investigation. In order to achieve the main challenging goal aimed at the structural optimization of these mechanical components, the numerical approach employed in this work is the finite element method. The finite element analysis is capable of handling the static problems associated with mechanical components having a complex three-dimensional geometry. The numerical analysis presented in this work is carried out with the aid of the commercial finite element software called ANSYS. This computational package has an array of effective computational tools for the pre and post-processing of the numerical data that are suitable for a detailed development of mechanical models of the structural components considered in this work. The verification of the methodology implemented in this investigation is done by means of a comparison between the results obtained with the numerical analysis developed in ANSYS (version 18.1) and a set of real measurements available from an experimental campaign.

E. Organization of the Manuscript

The remaining part of this paper is organized according to the following structure. In Section II, background material and the analytical formulation behind the finite element computational approach used in this paper are presented. In Section III, the general criteria for the structural redesign and optimization followed in this study are discussed. In Section IV, the numerical results developed in this work are illustrated and a discussion on the research insights as well as on the findings obtained in this paper is provided. In Section V, the summary of the work, the conclusions obtained in this investigation, and some suggestions on future directions of research are reported.

II. Mathematical Background on the Finite Element Method

In this section, background material on the application of the Finite Element Method (FEM) to the structural analysis of aircraft components is reported. First, the kinematics of isoparametric finite elements is discussed. Then, the

equations of motion of isoparametric finite elements are derived employing the D'Alembert-Lagrange principle of virtual work and considering a total Lagrangian formulation approach. Subsequently, the linear static problem of interest for the structural analysis carried out in this investigation is formulated.

A. Finite Element Kinematic Analysis

In the FEM discretization process, the spatial domain of the flexible body of interest is divided into small finite regions called elements as shown in Figure 1. The discretization in small elements allows for the use of low-order polynomials for describing the displacement field within the element by means of interpolating functions associated with a set of material points called nodes [66]. The preassigned interpolating polynomials define the kinematic properties of each element and, subsequently, are assembled using connectivity conditions at the finite element boundaries in order to construct the finite element mesh. By using the property of separation of variables, the element displacement field can be written as the product of one set of functions that depend only on the spatial coordinates and another set of functions which depend only on time [67]–[69]. Thus, the displacement field can be written in terms of the selected coordinates using the separation of variables and assuming that the continuum is divided into a large number of finite elements as follows:

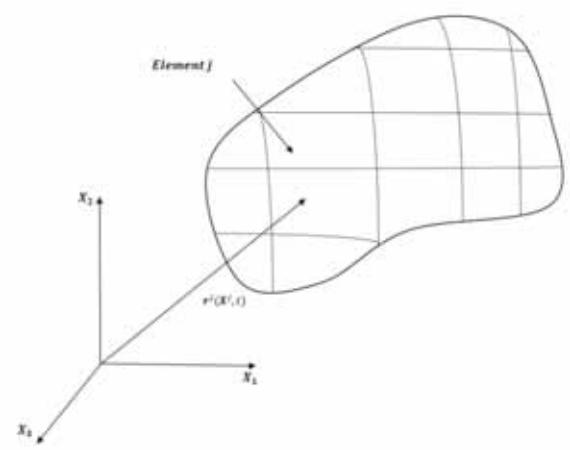

Fig. 1. Example of the finite element discretization.

$$\mathbf{r} = \mathbf{S}\mathbf{e} \tag{1}$$

where x, y, and z are the spatial coordinates defined in the element coordinate system, $\mathbf{x} = \begin{bmatrix} x & y & z \end{bmatrix}^T$ is the vector of the element spatial coordinates, t is time, $\mathbf{r} = \mathbf{r}(\mathbf{x}, t)$ is the element displacement field, $\mathbf{S} = \mathbf{S}(\mathbf{x})$ is the spatial-dependent matrix of the element shape functions, and $\mathbf{e} = \mathbf{e}(t)$ is the time-dependent vector of the element nodal coordinates. The separation of variables can be achieved by assuming that the position vector of an arbitrary material point can be written as a polynomial interpolation based on the spatial local coordinates of the element $\mathbf{x}$ and on the element nodal coordinates $\mathbf{e}$. In particular, the nodes are selected material points which can be associated with the configuration variables, such as displacements, rotations, and slopes, which are used as nodal coordinates [70]. Different element types employ a diverse set of shape functions and different kind of nodal coordinates. Some elements use only displacement coordinates whereas other ones use displacement and finite rotations. Isoparametric finite elements, on the other hand, make only use of displacements and, if necessary, slopes as generalized coordinates [71]. Therefore, isoparametric finite elements are able to capture straight as well as curved geometry by using the same set of shape functions changing only the value of the nodal coordinates. For example, the vector of nodal coordinates $\mathbf{e}$ of a linear hexahedral finite element, which is an important type of finite element employed in this investigation, is composed of the position vectors of the eight hexahedron vertex points and can be written as:

$$\mathbf{e} = \begin{bmatrix} \mathbf{r}_1^T & \mathbf{r}_2^T & \mathbf{r}_3^T & \mathbf{r}_4^T & \mathbf{r}_5^T & \mathbf{r}_6^T & \mathbf{r}_7^T & \mathbf{r}_8^T \end{bmatrix}^T \tag{2}$$

where $\mathbf{r}_k,\ k = 1, 2, \ldots, 8$ identifies the global position vector of the generic node k of the hexahedral finite element corresponding to one of its vertices. Consequently, the matrix of shape functions of the linear hexahedral element, which is a good example of an isoparametric finite element, is given by:

$$\mathbf{S} = \begin{bmatrix} S_1\mathbf{I} & S_2\mathbf{I} & S_3\mathbf{I} & S_4\mathbf{I} & S_5\mathbf{I} & S_6\mathbf{I} & S_7\mathbf{I} & S_8\mathbf{I} \end{bmatrix} \tag{3}$$

where $\mathbf{I}$ is the identity matrix and $S_k,\ k = 1, 2, \ldots, 8$ are the shape functions of the linear hexahedral element [72]. These shape functions are defined as:

$$\begin{cases} S_1 = \frac{1}{8}(1-\xi)(1-\eta)(1-\zeta) \\ S_2 = \frac{1}{8}(1+\xi)(1-\eta)(1-\zeta) \\ S_3 = \frac{1}{8}(1+\xi)(1+\eta)(1-\zeta) \\ S_4 = \frac{1}{8}(1-\xi)(1+\eta)(1-\zeta) \\ S_5 = \frac{1}{8}(1-\xi)(1-\eta)(1+\zeta) \\ S_6 = \frac{1}{8}(1+\xi)(1-\eta)(1+\zeta) \\ S_7 = \frac{1}{8}(1+\xi)(1+\eta)(1+\zeta) \\ S_8 = \frac{1}{8}(1-\xi)(1+\eta)(1+\zeta) \end{cases} \tag{4}$$

where ξ, η, and ζ are the natural coordinate of the hexahedron given by:

$$\begin{cases} \xi = \frac{x}{a} \\ \eta = \frac{y}{b} \\ \zeta = \frac{z}{c} \end{cases} \tag{5}$$

where a, b, c respectively denote half the length, half the width, and half the thickness of the hexahedral element. In general, the accuracy of the finite element analysis depends on the selection of the number of nodal points and the number of coordinates at each node. With a simple and general continuum mechanics description of the motion of an infinitesimal volume, the vector of nodal coordinates can be selected in the three-dimensional analysis to consist of three

translational coordinates and the nine components of the position vector gradients. When the nine slope coordinates are used in conjunction with the three translational coordinates, the three rigid rotations and the six deformation modes of an infinitesimal cube associated with a general nodal point are embedded in the nine components of the slopes.

B. Nonlinear Finite Element Dynamic Analysis

In the FEM, the dynamic equations of an isoparametric finite element can be readily obtained starting from the basic principles of analytical dynamics and employing an analytical approach based on the general theory of continuum mechanics [73]. To this end, one can define the matrix of position vector gradients as follows:

$$\begin{aligned}\mathbf{J} = \frac{\partial \mathbf{r}}{\partial \mathbf{r}_0} = \frac{\partial \mathbf{r}}{\partial \mathbf{X}} = \left[\begin{array}{ccc} \frac{\partial \mathbf{r}}{\partial X} & \frac{\partial \mathbf{r}}{\partial Y} & \frac{\partial \mathbf{r}}{\partial Z} \end{array} \right] \\ = \left[\begin{array}{ccc} \mathbf{r}_X & \mathbf{r}_Y & \mathbf{r}_Z \end{array} \right]\end{aligned} \tag{6}$$

where $\mathbf{r}$ identifies the element position field in the deformed current configuration and $\mathbf{r}_0 = \mathbf{X}$ denotes the element position field in the curved reference configuration [74]. In fact, the curved reference configuration can be easily established by defining a particular vector of nodal coordinates $\mathbf{e}_0$ associated with the reference configuration to yield:

$$\mathbf{X} = \mathbf{r}_0 = \mathbf{S}\mathbf{e}_0 \tag{7}$$

However, it is more convenient to express the matrix of position vector gradients $\mathbf{J}$ in terms of matrix quantities referred to the straight configuration in which, by definition, the element position field is identical to its local vector of Cartesian coordinates $\mathbf{x}$. For this purpose, one can write:

$$\mathbf{J} = \frac{\partial \mathbf{r}}{\partial \mathbf{r}_0} = \frac{\partial \mathbf{r}}{\partial \mathbf{x}} \frac{\partial \mathbf{x}}{\partial \mathbf{r}_0} = \left(\frac{\partial \mathbf{r}}{\partial \mathbf{x}} \right) \left(\frac{\partial \mathbf{r}_0}{\partial \mathbf{x}} \right)^{-1} = \mathbf{J}_e \mathbf{J}_0^{-1} \tag{8}$$

where:

$$\mathbf{J}_e = \frac{\partial \mathbf{r}}{\partial \mathbf{x}}, \quad \mathbf{J}_0 = \frac{\partial \mathbf{r}_0}{\partial \mathbf{x}} \tag{9}$$

where $\mathbf{J}_e$ is the matrix of the position vector gradients in the current configuration computed with respect to the coordinate lines of the straight configuration and $\mathbf{J}_0$ is the matrix of the position vector gradients in the reference configuration computed with respect to the coordinate lines of the straight configuration [75]. On the other hand, one can easily write the virtual change of the element position field exploiting the property of separation of variables as follows:

$$\mathbf{r} = \mathbf{S}\mathbf{e} \quad \Rightarrow \quad \delta\mathbf{r} = \mathbf{S}\delta\mathbf{e} \tag{10}$$

where $\delta\mathbf{e}$ denotes a virtual change of the vector of the element nodal coordinates. In a similar manner, the virtual changes of the element gradient fields can be expressed as:

$$\left\{ \begin{array}{l} \mathbf{r}_x = \mathbf{S}_x\mathbf{e} \\ \mathbf{r}_y = \mathbf{S}_y\mathbf{e} \\ \mathbf{r}_z = \mathbf{S}_z\mathbf{e} \end{array} \right. \quad \Rightarrow \quad \left\{ \begin{array}{l} \delta\mathbf{r}_x = \mathbf{S}_x\delta\mathbf{e} \\ \delta\mathbf{r}_y = \mathbf{S}_y\delta\mathbf{e} \\ \delta\mathbf{r}_z = \mathbf{S}_z\delta\mathbf{e} \end{array} \right. \tag{11}$$

where $\mathbf{S}_x$, $\mathbf{S}_y$, and $\mathbf{S}_z$ represent the spatial derivatives of the matrix of element shape functions computed with respect to the element Cartesian coordinates x, y, and z. Considering a total Lagrangian formulation approach [76], the D'Alembert-Lagrange principle of virtual work can be written as follows:

$$\delta W_i + \delta W_s + \delta W_e = 0 \tag{12}$$

where δW_i identifies the virtual work of the element inertia forces, δW_s represents the virtual work of the element elastic forces, and δW_e denotes the virtual work of the element external forces. The virtual work of the element inertia forces can be expressed as follows:

$$\delta W_i = -\int_V \rho \ddot{\mathbf{r}}^T \delta\mathbf{r} \, |\mathbf{J}_0| \, dV \tag{13}$$

where ρ is the element mass density defined in the reference configuration, $\ddot{\mathbf{r}}$ is the global acceleration of a generic material point that belongs to the finite element, $\delta\mathbf{r}$ is the virtual change of the absolute position vector of the same point, $|\mathbf{J}_0|$ is the determinant of the matrix of the element position vector gradients defined in the reference configuration, and V is the element volume in the straight configuration. Employing the element kinematic equations and the definition of the virtual variation, the virtual work of the element inertia forces can be explicitly rewritten as:

$$\delta W_i = -\ddot{\mathbf{e}}^T \int_V \rho \mathbf{S}^T\mathbf{S} \, |\mathbf{J}_0| \, dV \delta\mathbf{e} = -(\mathbf{M}\ddot{\mathbf{e}})^T \delta\mathbf{e} \tag{14}$$

where:

$$\mathbf{M} = \int_V \rho \mathbf{S}^T\mathbf{S} \, |\mathbf{J}_0| \, dV \tag{15}$$

where $\mathbf{M}$ represents the element mass matrix that is a constant positive-definite symmetric matrix. A standard finite element assembly procedure can be used to define the mesh mass matrix $\mathbf{M}_b$ starting from the mass matrix $\mathbf{M}$ of each finite element. The virtual work of the element elastic forces is given by:

$$\delta W_s = -\int_V \boldsymbol{\sigma}_v^T \delta\boldsymbol{\varepsilon}_v \, |\mathbf{J}_0| \, dV \tag{16}$$

where $\boldsymbol{\sigma}_v$ represents the second Piola-Kirchhoff stress tensor expressed using the Voigt vector notation and $\delta\boldsymbol{\varepsilon}_v$ denotes the virtual variation of the Green-Lagrange strain tensor expressed using the Voigt vector notation. Since the kinematic description of isoparametric finite elements is general and allows for correctly representing the rigid body motion, general constitutive laws can be employed in the formulation of the elastic forces. For example, the Voigt form of the second Piola-Kirchhoff stress tensor $\boldsymbol{\sigma}_v$ can be calculated from the Voigt form of the Green-Lagrange strain tensor $\boldsymbol{\varepsilon}_v$ considering a linear elastic constitutive model:

$$\boldsymbol{\sigma}_v = \mathbf{E}_v\boldsymbol{\varepsilon}_v \tag{17}$$

where $\mathbf{E}_v$ is the matrix of elastic coefficients expressed in the Voigt form which includes the element Young modulus E and the element Poisson ratio ν. On the other hand, the Green-Lagrange strain tensor $\boldsymbol{\varepsilon}$ can be readily obtained from the deformation gradient tensor $\mathbf{J}$ as:

$$\boldsymbol{\varepsilon} = \frac{1}{2}\left(\mathbf{J}^T\mathbf{J} - \mathbf{I}\right) \tag{18}$$

By using the element kinematic equations and the definition of the virtual variation, the virtual work of the element elastic forces can be explicitly reformulated as follows:

$$\delta W_s = -\int_V \boldsymbol{\sigma}_v^T \frac{\partial \boldsymbol{\varepsilon}_v}{\partial \mathbf{e}} \, |\mathbf{J}_0| \, dV \delta\mathbf{e} = \mathbf{Q}_s^T \delta\mathbf{e} \tag{19}$$

where:

$$\mathbf{Q}_s = -\int_V \left(\frac{\partial \boldsymbol{\varepsilon}_v}{\partial \mathbf{e}} \right)^T \boldsymbol{\sigma}_v \, |\mathbf{J}_0| \, dV \tag{20}$$

where $\mathbf{Q}_s$ denotes the vector of the element generalized elastic forces which must be evaluated numerically employing numerical quadrature formulas such as, for example, the Gauss quadrature procedure because this vector is a highly nonlinear function of the element nodal coordinates. A standard finite element assembly procedure can be employed to obtain the mesh generalized elastic force vector $\mathbf{Q}_{s,b}$ starting from the generalized elastic force vector $\mathbf{Q}_s$ of each finite element. The virtual work of the element external forces can be written as:

$$\delta W_e = \int_V \mathbf{f}_e^T \delta \mathbf{r} \, |\mathbf{J}_0| \, dV \tag{21}$$

where $\mathbf{f}_e$ is a vector of distributed external forces such as the applied distributed loads and the gravity force. Considering the element kinematic equations and the definition of the virtual variation, the virtual work of the element external forces can be explicitly calculated as:

$$\delta W_e = \int_V \mathbf{f}_e^T \mathbf{S} \, |\mathbf{J}_0| \, dV \delta \mathbf{e} = \mathbf{Q}_e^T \delta \mathbf{e} \tag{22}$$

where:

$$\mathbf{Q}_e = \int_V \mathbf{S}^T \mathbf{f}_e \, |\mathbf{J}_0| \, dV \tag{23}$$

where $\mathbf{Q}_e$ identifies the external force vector applied to the element nodal coordinates. A standard finite element assembly procedure can be used for deriving the mesh external force vector $\mathbf{Q}_{e,b}$ starting from the external force vector $\mathbf{Q}_e$ of each finite element. Finally, the formulation of the principle of virtual work in the case of the unconstrained motion of the finite element leads to:

$$\left(-\mathbf{M}\ddot{\mathbf{e}} + \mathbf{Q}_s + \mathbf{Q}_e\right)^T \delta \mathbf{e} = 0 \tag{24}$$

where:

$$\forall \delta \mathbf{e} \quad \Rightarrow \quad \mathbf{M}\ddot{\mathbf{e}} = \mathbf{Q}_s + \mathbf{Q}_e \tag{25}$$

which represents a nonlinear set of Ordinary Differential Equations (ODEs). As mentioned before, the equations of motion of the continuum body of interest can be readily obtained by using a standard finite element assembly procedure since the elements that form the continuum domain must be properly connected at the nodal points. Denoting with $\mathbf{e}_b$ the total vector of nodal coordinates associated with the finite element mesh obtained by assembling the nodal coordinate vectors $\mathbf{e}$ of each element, one can readily write the complete set of equations of motion of the continuum body as follows:

$$\mathbf{M}_b \ddot{\mathbf{e}}_b = \mathbf{Q}_{s,b} + \mathbf{Q}_{e,b} \tag{26}$$

where $\mathbf{M}_b$, $\mathbf{Q}_{s,b}$, and $\mathbf{Q}_{e,b}$ respectively represents the mesh mass matrix, the mesh generalized elastic force vector, and the mesh generalized external force vector. The equations of motion of the finite element mesh constructed by using isoparametric finite elements can be numerically solved employing a non-incremental solution procedure.

C. Linear Finite Element Static Analysis

In static problems, one is interested in computing the steady-state solutions of the equations of motion, namely the equilibrium configuration reached by the continuum body when a set of constant loading conditions is applied [77]. For this purpose, one can neglect the inertia effects in the equations of motion to yield:

$$\mathbf{Q}_{s,b} + \mathbf{Q}_{e,b} = \mathbf{0} \tag{27}$$

Furthermore, in structural engineering problems, the attention is mainly focused on the behavior of the mechanical system of interest when small perturbations from the equilibrium configuration occur because of external factors such as the operative loading conditions. In this important scenario, which is of interest for this investigation, one can reformulate the problem at hand in linear terms and consider the stiffness matrix arising from the linearization of the body generalized elastic force vector. By doing so, one obtains:

$$\mathbf{Q}_{s,b} \approx -\mathbf{K}_{s,b}\mathbf{e}_b \tag{28}$$

which leads to:

$$-\mathbf{K}_{s,b}\mathbf{e}_b + \mathbf{Q}_{e,b} = \mathbf{0} \quad \Leftrightarrow \quad \mathbf{K}_{s,b}\mathbf{e}_b = \mathbf{Q}_{e,b} \tag{29}$$

where $\mathbf{K}_{s,b}$ represents the stiffness matrix of the finite element mesh that characterizes the linear structural problem for the continuum body of interest. By solving the system of linear equations obtained assuming a proper set of boundary conditions and external forces, one obtains the vector of nodal coordinates $\mathbf{e}_b$ that identifies the equilibrium configuration of the mechanical system of interest. Employing the vector of nodal coordinates $\mathbf{e}_b$ and considering the continuum mechanics approach described before, one can readily compute the symmetric Green-Lagrange strain tensor $\boldsymbol{\varepsilon}$ and the symmetric second Piola-Kirchhoff stress tensor $\boldsymbol{\sigma}$ which represent important physical quantities employed for performing the structural analysis.

III. Redesign and Structural Optimization

In this section, a simple structural optimization algorithm used for aiding the redesign of the aircraft components is described. The optimization process consisted of testing different materials that satisfy the mechanical requirements of the components analyzed in this investigation [78]. In this research work, the optimization approach used for material selection is aimed at achieving an economic lightweight design and a multi-objective optimization scheme based on trade-off surfaces is implemented. An objective function for the composite materials is formulated in such a way that the minimum of the function defines the most preferable solution. To do this, a locally linear utility function denoted with V is used and is defined as follows:

$$V = \sum_{i=1}^{M} \alpha_i P_i \tag{30}$$

where M is the number of objectives, two for the cases considered in this work, and the coefficients α_i are constant weights called exchange coefficients that can depend on the performance metrics P_i when the search space is large. The utility function V reflects the value of each solution and the exchange constants convert units of performance into the unit of utility. This process allows for comparing the weight of the materials with the price of those materials. The selected material is chosen in order to compare each material with the other ones by means of the performance metrics. The properties implemented in the optimization approach employed in

this investigation are the relations weight/mechanical resistance and the weight/production costs [79]–[81]. Therefore, the performance metrics are defined following two principal objectives: a) minimizing the total mass and b) minimizing the total cost. A square matrix is generated by the comparison process. The columns of this square matrix represent the dominance of each material in a determined performance metrics. This index is equal to the number of objectives when a material dominates the other ones used for computing the corresponding performance metrics. The schematic flowchart shown in Figure 2 represents the steps followed for the logic process of the structural optimization algorithm used in this work.

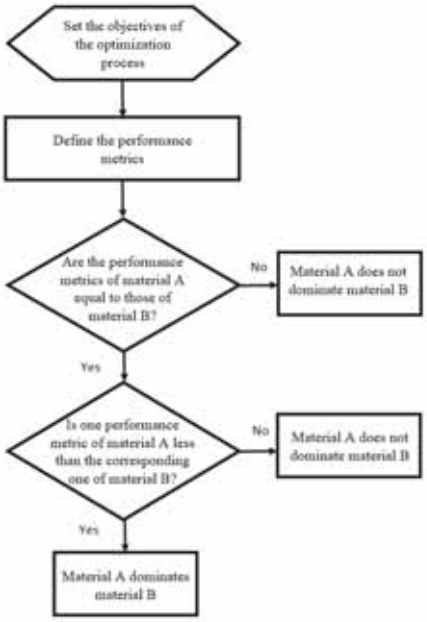

Fig. 2. Optimization flowchart.

For minimizing the cost C, which is in units of a given currency, the following simple procedure can be used. A change in the cost C produces a unit change in the utility function V:

$$\alpha_1 = \left(\frac{\partial V}{\partial C}\right)_{P_1,\ldots,P_i,\ldots} = 1 \tag{31}$$

where the utility function V is redefined in order to include the cost C as follows:

$$V = C + \alpha_1 P_1 + \ldots + \alpha_i P_i + \ldots \tag{32}$$

If a previously selected material M is substituted with a new material M_o, based on the cost C and having a minimum weight with maximum stiffness quantified by the ratio ρ/E, the substitution is viable if the value V of the previously selected material M is less than V_o of the new material M_o. This leads to:

$$V - V_o = (C - C_o) + \alpha\,(P - P_o) \leq 0 \tag{33}$$

Or equivalently:

$$\Delta V_o = \Delta C + \alpha \Delta P \leq 0 \tag{34}$$

From which one can deduce that:

$$\frac{\Delta P}{\Delta C} \leq -\frac{1}{\alpha} \tag{35}$$

In Figure 3, the performance metric P and the cost C are shown. The actual material is centered at (P_o, C_o), the line trough M_o is calculated using Equation (34) with the equality sign. The materials that lie on this line will have the same

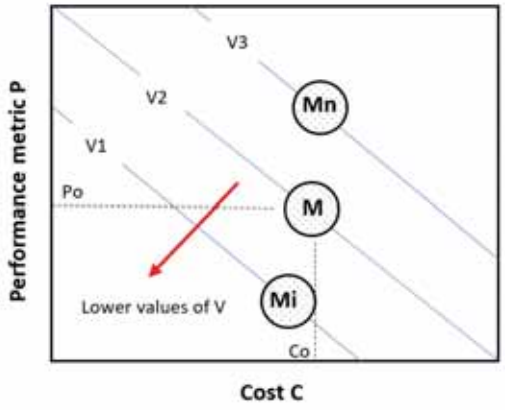

Fig. 3. Trade-off between cost and stiffness - M_n is not a suitable substitute for M, Material M_i is a viable substitute for M because it has a lower value of ΔV.

value of V, while the materials above this line will have a higher value of V and materials below this line will have a lower value of V, a necessary condition for the substitution [82].

IV. Numerical Results and Discussion

In this section, the numerical results obtained for the finite element models developed in this paper are presented. Subsequently, the numerical solutions found in this investigation are analyzed using different failure criteria. A comparison with the numerical results and the set of experimental data available is performed in this section as well. The case study considered in this investigation for the structural redesign and optimization process involves two important aeronautical components, namely the bulkhead and the flaps. The displacement field across the vertical axis of the mechanical components considered in this study is obtained using the finite element analysis and the numerical results are compared with a set of experimental data available for the flaps. By doing so, an estimation of the error associated with the finite element model of the flaps is obtained. In the case of the bulkhead, on the other hand, there is no experimental data available. Therefore, in the finite element analysis of the bulkhead, a multi-point constraint and simply pinned supports are considered in order to simulate the interaction with the fuselage of the aircraft. However, the numerical results obtained for the bulkhead lead to a realistic behavior of this structural component, thereby allowing for performing a redesign of an optimized structural part. In order to perform the static analysis, the simulations were carried out in this investigation using the commercial finite element software called ANSYS [83]. This software provides the tools for generating the finite element mesh and for performing the

static analysis of composite materials with high accuracy. Furthermore, a precise direction of the fibers and a high-quality mesh for complex three-dimensional geometry can be obtained in this computational framework. Considering different loading scenarios, the strain and stress fields are computed in ANSYS for each mechanical component performing a static analysis. In particular, the critical points corresponding to the maximum values of the strains and stresses were found in the strain and stress fields. Another important aspect considered in this research work is the possibility of the failure of the structural components. For this purpose, different failure criteria are employed for the flaps and the bulkhead. The failure criterion used for the flap made of aluminum is the Von Mises yield criterion. On the other hand, in the case of the flap and the bulkhead made of composite materials, the failure criteria considered are the maximum principal stress and the Tsai-Hill theory. The numerical results arising from the application of the failure criteria mentioned before demonstrated that the materials and the ply sequence considered in the optimized redesign of the components analyzed in this work are suitable for bearing the prescribed loading conditions.

A. Bulkhead

In the aircraft system analyzed in this work, the fuselage is divided into two parts which are joined together along the vertical plane by means of the bulkheads. In Figure 4, the typical fuselage components are represented [81]. The main bulkhead must support the undercarriage and the engine. Therefore, the bulkhead is a structural component that plays a fundamental role in the design and optimization of an aircraft system. In this study, it is desired to change the material of this important component in order to reduce the manufacturing time and the total weight of the aircraft. To achieve this goal, the performance of pre-impregnated carbon fiber reinforced polymers is analyzed.

In the original design solution, the bulkhead was built with a series of carbon fiber sheets which reinforce various areas of this component according to the mechanical resistance required in the design. Figure 5 shows some of the layers of the material used in the original design solution. However, the problem of the material used in the original design solution is its weight during the operative conditions and the molding time required in the manufacturing process. In particular, the component with this material weighs between $6.5\ (\mathrm{kg})$ and $9.0\ (\mathrm{kg})$. In fact, the manual application of the resin generates great differences between the final weights of each component. This can be solved by means of the use of prepreg materials. The main advantages of using pre-impregnated composite fibers are listed below:

- 1. Greater resistance because the resin is applied in the right proportion. In weight, the percentage should be $50/50$ with the fabric, sometimes less. The excess resin obtained in hand laminates increases the brittleness of the material.
- 2. There are greater uniformity and repeatability of the manufacturing process. The differences between thicknesses and weights of the components are considerably reduced.
- 3. Curing time is reduced. After the application of heat, the component is ready to be reused. There is also a reduction in the resin expense.

However, the main disadvantage of the prepreg is its cost. Even taking into account the savings in the curing and the resin costs, the prepreg continues to have a higher cost. In this work, on the other hand, a total of 8 plies of fiber carbon reinforced prepreg with the orientation code $[+45, 0, 0, +45]\, s$ was used in the finite element model. The numbers reported in the string that characterizes the orientation code of a given composite material are used to specify the orientation angles of each layer of the composite fibers, whereas the letter 's' means that the sequence is repeated in a symmetric fashion. The mechanical properties of the material considered in this investigation are reported in Table I.

TABLE I
PHYSICAL PROPERTIES OF THE MATERIAL USED IN THE BULKHEAD.

Material Properties	
Elastic Modulus, E_{xx}	48.26 GPa
Elastic Modulus, E_{yy}	55.16 GPa
Poisson Ratio, v_{xy}	0.005
Shear Modulus, τ_{xy}	4067.91 MPa
Shear Modulus, τ_{xz}	2847.53 MPa
Shear Modulus, τ_{zy}	2847.53 MPa
Density, ρ	15.22E03 $\mathrm{kg/m^3}$

B. Flap

The wing flaps of the aircraft provide the necessary increase of lift for takeoff and landing [81]. In Figure 6, the typical wing components are represented. The flap considered in this study was initially designed and prototyped using the aluminum as the material. However, in a subsequent new design phase, it was decided to use composite materials. The main objective is to reduce weight, thereby reducing energy consumption, in order to increase the autonomy of the aircraft.

In the design phase, two types of flaps with different materials are developed. The first type of flap is completely made with aluminum while the second type of flap makes use of various composite materials.

1) Flap made with Aluminum: The first type of flap is made of an aluminum alloy having an elastic modulus $E = 71000\ (\mathrm{MPa})$. The first type of flap is more complex than the second type of flap made with the composite materials because it has more structural parts. Without taking into account screws, which were removed to simplify the finite element model, the first type of flap has a weight of $0.342\ (\mathrm{kg})$. Figure 7 shows the original model for the first type of flap.

2) Flap made with Composite Materials: The second type of flap is made of composite materials and it has a simpler mechanical structure. The skin is made with two sheets of unidirectional carbon fiber, while the structural components are made with glass fiber and a low-density foam core. The total weight of this flap is $0.281\ (\mathrm{kg})$. Figure 8 shows the redesigned model. Table II shows some elastic properties of the materials used.

C. Replication of Results

In this subsection, the findings obtained by means of the finite element method used for performing the structural

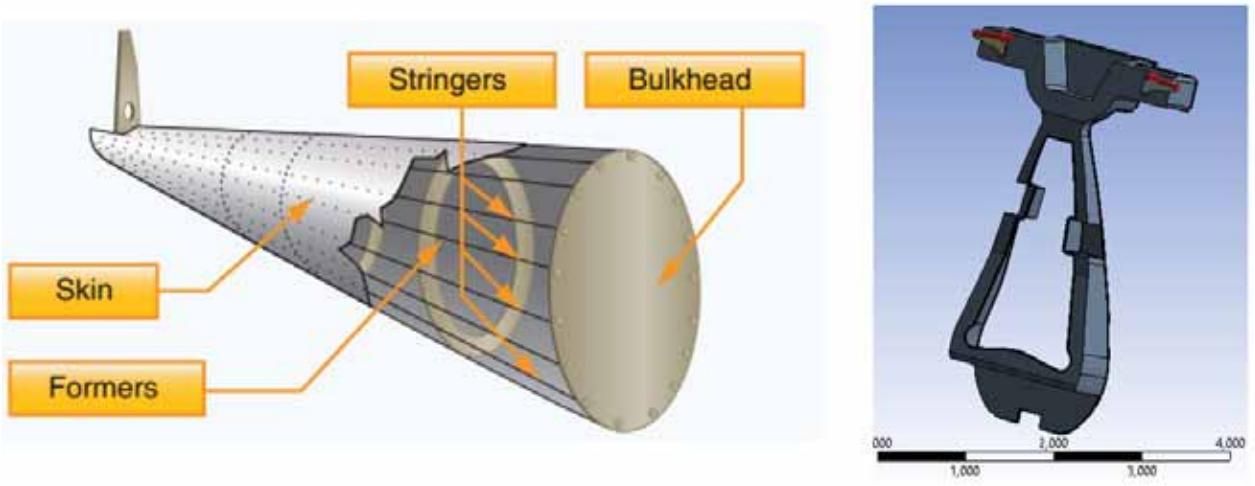

Fig. 4. Left: Fuselage main components, Right: Bulkhead.

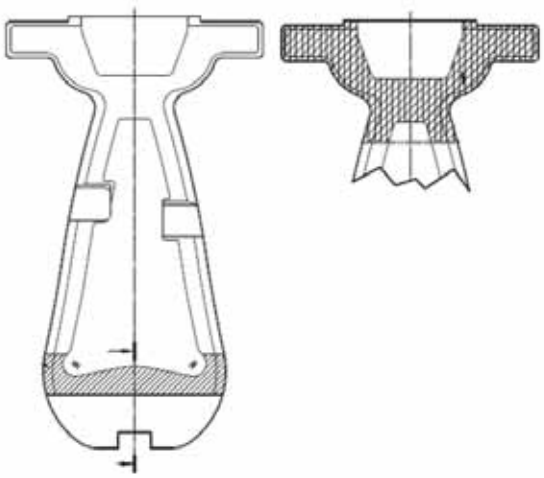

Fig. 5. Bulkhead before the redesign.

TABLE II
PHYSICAL PROPERTIES OF THE COMPOSITE MATERIALS USED IN THE FLAP.

Materials Properties		
UD Fiber Carbon	**Epoxy glass wet**	**Foam**
Ex 209000 MPa	Ex 35000 MPa	Ex 70 MPa
Ey 9450 MPa	Ey 9000 MPa	Ey 70 MPa
Ez 9450 MPa	Ez 9000 MPa	ν 0.3

redesign and optimization of the aeronautical components of interest for this investigation are reported. This subsection contains material and data to further understand and replicate the proposed approach.

1) Finite Element Types: In the structural model developed in ANSYS, the first type of finite element used for meshing the geometric model made with composite materials is SHELL181. The finite element SHELL181 is a four-node shell element with six degrees of freedom at each node, namely three translations in the x, y, and z directions, and three rotations about the axes x, y, and z. In structural engineering applications, several composite structures are built using plate or shell elements. This is because the structure works more efficiently when it carries membrane loads and because the thick laminates are difficult to produce. According to the definitions commonly accepted in the finite element literature, the plate elements can be considered as a particular case of shell elements in which there is no initial curvature [82]. The plate elements used in the finite element analysis implemented in ANSYS have only three degrees of freedom per node, namely the three nodal translations [84]. In the computation of the generalized elastic forces, some assumptions must be done in order to reduce the governing equations from 3D to 2D. To this end, the Kirchhoff theory is the most used theory because it can be written in terms of only one field variable, namely the transverse deflection of the shell [85]. On the other hand, the second finite element type used in this work for meshing the other structural components made with isotropic materials is the solid (brick) element. In particular, the hexahedral element used in ANSYS is called SOLID187. The finite element SOLID187 is defined by ten material nodes having three degrees of freedom at each node that are the nodal translations in the directions x, y, and z. In ANSYS, this type of finite element allows for using several interesting features such as the plasticity, hyper-elasticity, creep, stress stiffening, large deflection, and large strain capabilities [86]. It also has a mixed formulation capability for simulating deformations of nearly incompressible elasto-plastic materials and fully incompressible hyper-elastic materials. Furthermore, the contact elements are used in ANSYS to define the behavior of the surfaces in contact. The contact element used in this research work is CONTACT174. The contact element CONTACT174 is used to represent the contact as well as the sliding between 3D target surfaces and a deformable surface defined by this element. The element is applicable to 3D structural components and to perform coupled-field contact analysis. It can be used for both pair-based contact and general contact. The contact element considered in this work has the same geometric characteristics of the face of the solid or shell finite element with which it is connected to. The contact occurs when the element surface penetrates

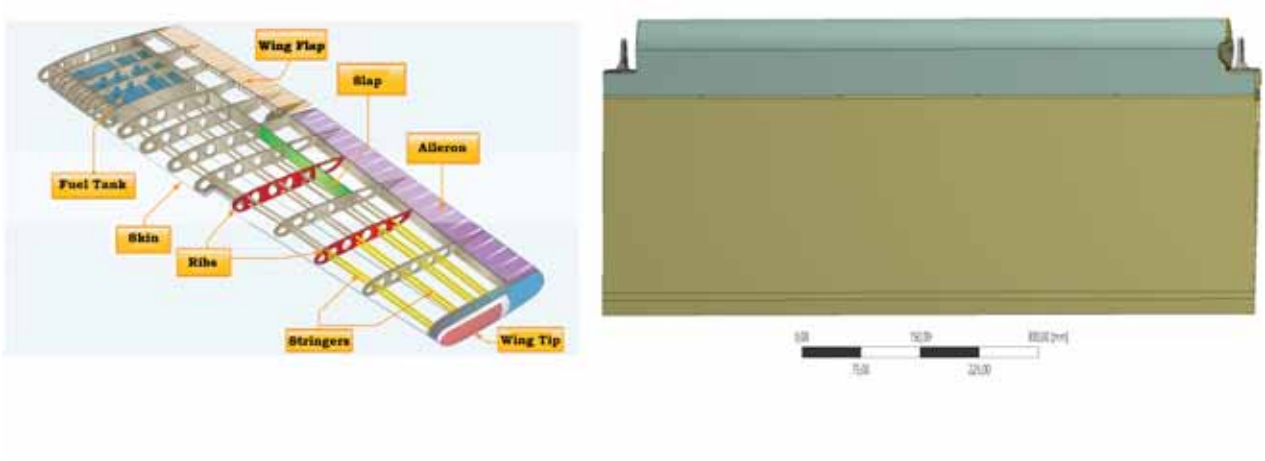

Fig. 6. Left: Wing main components, Right: Flap.

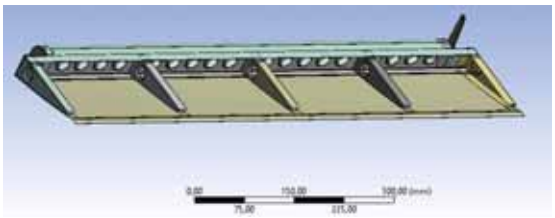

Fig. 7. Flap made with aluminum.

TABLE III
FINITE-ELEMENT STATIC ANALYSIS CARRIED OUT OVER THE BULKHEAD.

Model Parameters	
Active Bodies	3
Number of Nodes	51905
Number of Elements	56571
Stiffness Behavior	Flexible
Max. Structural Error	1.242
Min. Structural Error	9.381E-04

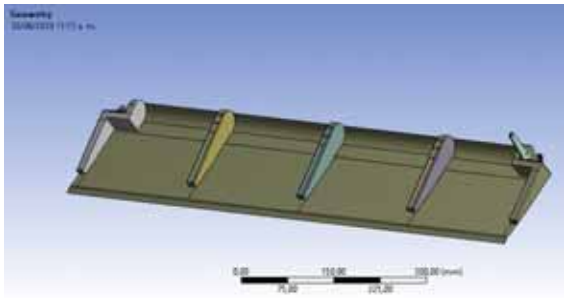

Fig. 8. Flap made with composite materials.

an associated target surface. Due to the complexity of the geometry of the models, a behavior called 'No Separation' was employed, thereby avoiding the separation between the surfaces in contact, and, on the other hand, allowing very small slides and penetrations that help to reduce computer time.

2) Stress and Strain Fields of the Bulkhead: In the bulkhead, the stress and strain fields are calculated in order to verify if the geometric shape and the direction of the fibers considered in the configuration at hand exceed the resistance limits of the selected material. Furthermore, different failure criteria are used for evaluating in a conservative manner the response of the bulkhead to the external loads to which it is subjected. The summary of the finite element analysis carried out in this subsection is presented in Table IV-C2. In particular, the stresses of each ply and of the entire bulkhead are calculated. The maximum stress observed is $116.13\ (\mathrm{MPa})$. This value is sufficiently smaller than the yield strength of the laminated in the principal directions. However, a failure criterion for composite materials is applied to verify the viability and the robustness of the current design. Figure 9(a) shows the stress field of the bulkhead considering the equivalent Von Mises stress expressed in mega-Pascals. Also, the strain limits are important values to take into account in the design process involving composite materials. In particular, the admissible strain values are larger than the maximum strain calculated in the present finite element analysis. Figure 9(b) shows the total strain field of the bulkhead.

3) Failure Criteria: Considering the available data for the strength of the materials of interest for this study, three failure criteria are taken employed for evaluating the failure modes of the bulkhead. The first criterion considered is the maximum strain criterion [87]. The maximum strain criterion is not a conservative criterion, but it is useful for evaluating one of the material resistance limits. Figures 10(a) and 10(b) respectively show the failure strain and the failure stress of the bulkhead. Figure 10(a) shows a low value of the strain for this failure criterion. This phenomenon is due to the large admissible values of the material considered in this study. The maximum strain criterion is a non-interactive failure criterion. In other words, this criterion does not consider any interaction between the different components. For this reason, two additional failure criteria are considered in this work. The prepreg used in the present design has quite large strain limits. Since this composite material is woven, these properties are repeated in its principal directions along

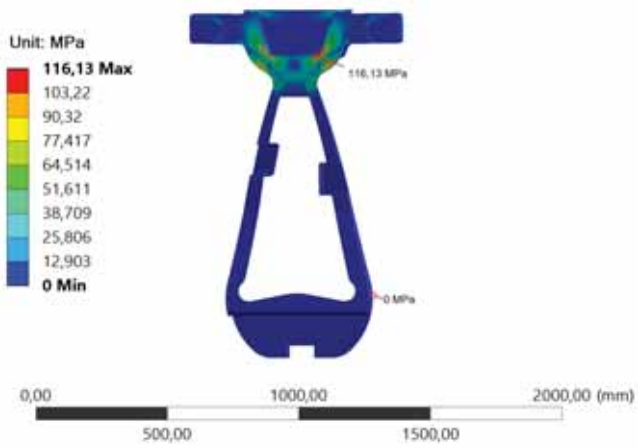

(a) Bulkhead stress.

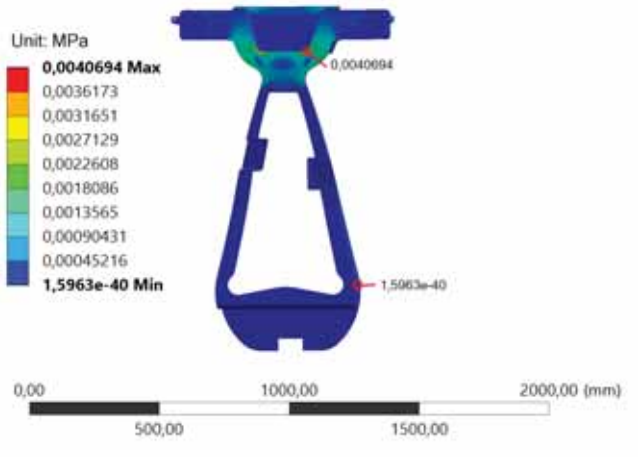

(b) Bulkhead strain.

Fig. 9. Stress and strain fields of the bulkhead.

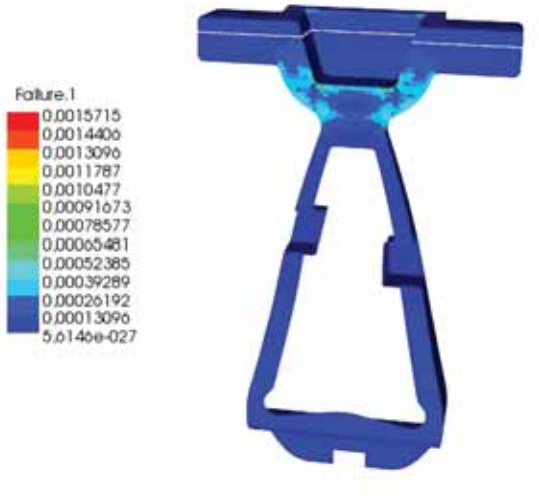

(a) Maximum strain.

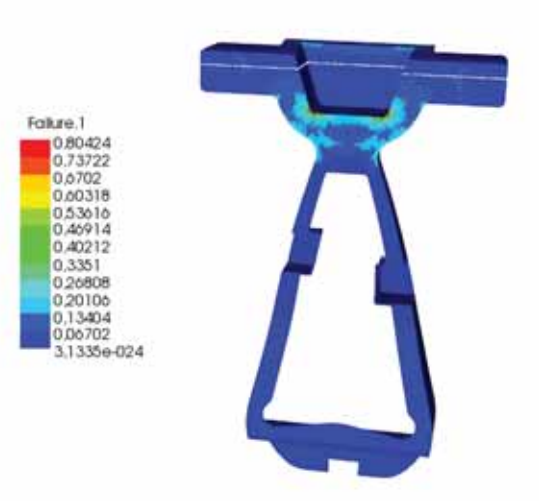

(b) Maximum stress.

(c) Tsai-Hill coefficient.

Fig. 10. Failure criterion implemented for the bulkhead.

the plane. The only problem that this configuration brings, and that of the laminates in general, is when out-of-plane stresses are generated since in that direction the resistance is remarkably low. The maximum stress criterion is similar to the criterion used for isotropic materials. Stresses in principal direction are compared with the tensile or compression strength in those directions. The inverse of the maximum of the values obtained from the previous relationship is the failure mode. The limitation of this criterion, similarly to the previous one, is the non-interaction between efforts in different directions, which is critical for this type of material. On the other hand, the Tsai-Hill criterion is an interactive failure criterion [88]. It is a conservative criterion and it is often used in engineering applications since only the resistance properties in the main directions are needed. Figure 10(c) shows that according to the Tsai-Hill criterion the failure coefficient is very close to 1, which is its maximum value. The main problem with the Tsai-Hill criterion is that it is unable to capture the difference between compression and tension stresses. In order to solve this problem, this criterion is commonly replaced by that of Tsai-Wu. However, the constants necessary to apply the theory of Tsai-Wu are not always available since they require equi-biaxial tests which are not simple to perform. Another problem with all the failure criteria used in this work is that they do not predict

TABLE IV
FINITE-ELEMENT STATIC ANALYSIS CARRIED OUT OVER THE FLAP MADE WITH ALUMINUM.

Model Parameters	
Active Bodies	17
Number of Nodes	1669290
Number of Elements	515305
Stiffness Behavior	Flexible
Max Structural Error	2.7155
Min Structural Error	8.38E-03

the failure mode as most of the available failure criteria. In principle, a delamination analysis performed by means of fracture mechanics can provide more accurate results but this issue is outside the scope of the present study.

4) Stress Field of the Flap made with Aluminum: Both the types of flap analyzed in this study by using a finite element approach have the same set of boundary conditions as shown in Figure 11. In particular, each type of flap is supported by

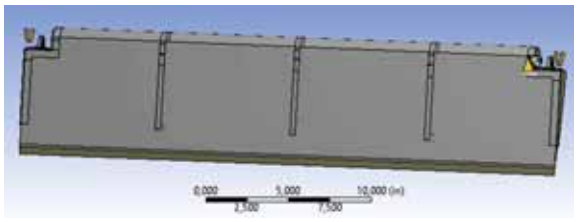

Fig. 11. Flap boundary conditions.

two bearings that are incorporated laterally and allow free local rotations of the structure. The flap is subsequently fixed by a component joined to the angle of attack. A vertical force is applied to the skin of the flap. The value of this load is modified nine times for evaluating the behavior of the flap in different operative conditions. The force is distributed along the skin (green) and at the angle of attack (red) as it is shown in Figure 12. The values of the external forces used for each

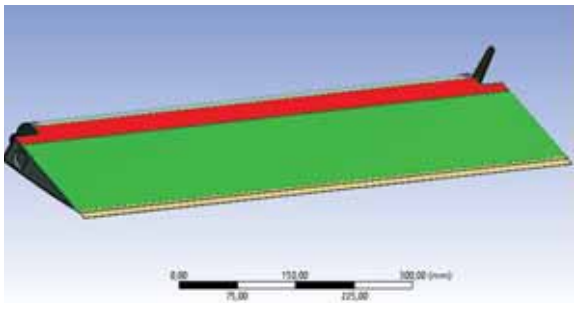

Fig. 12. Forces applied to the flap made with aluminum.

simulation vary from 10 (N) to 90 (N). Table IV shows the principal characteristics of the finite element analysis carried out for the flaps. Additionally, a study of the convergence of the mesh is carried out in order to determine the appropriate number of elements to use in the finite element analysis. By doing so, the equivalent Von Mises stresses are calculated. Figure 13 shows the stress distribution of the flap. The maximum and minimum stresses are also indicated in this figure. The maximum stress is calculated for different loading conditions, from 10 (N) to 90 (N). In the critical load

TABLE V
SECURITY FACTOR CALCULATED FOR THE FLAP MADE WITH ALUMINUM.

Security Factor									
Error	13	4.1	2.6	2.2	1.9	1.7	1.5	1.2	1.1
Load [N]	10	20	30	40	50	60	70	80	90

TABLE VI
ESTIMATED ERROR FOR THE FLAP MADE WITH ALUMINUM.

Estimated Error					
Error	20.4	11.5	27.0	23.5	16.0
Step	1	2	3	4	5
Error	17.4	14.6	16.1	15.7	18.0
Step	6	7	8	9	**Avg.**

condition, the Von Mises stress is 390.14 (MPa), which generates a security factor of approximately 1.1 considering a strength yield of 450 (MPa) as shown in Table IV-C4. Figure 14 shows the maximum Von Mises stresses for each load.

5) Vertical Displacement of the Flap made with Aluminum: A deformation measurement is made in the vertical direction at a specific point of interest of the flap. The point has coordinates $(470, 170)$ considering as reference the lower left corner of the component. Figure 15 shows the location of the point of interest. Ten measurements of deformation with respect to the vertical axis are made at this point considering the various simulation scenarios taken into account. The maximum displacement experimentally measured is 0.69(mm), while in the numerical simulation a maximum displacement of 0.81(mm) is calculated. In general, their values are very close and the average error is about 20%. In particular, the maximum difference between the numerical and the experimental displacements is 0.12(mm). Figure 16 shows the comparison of the displacements experimentally measured and numerically calculated. Table VI shows the values of the error for each loading condition.

6) Stress Field of the Flap made with Composite Materials: The same procedure described above is carried out with the flap made of composite materials. The numerical data of the finite element analysis performed in this scenario are shown in Table VII. Figure 17 shows the stress field over the flap made with composite materials. However, these stresses cannot be evaluated with a failure criterion because there is no available data for the strength of the material. Furthermore, the maximum stress is calculated for each load value applied. The maximum stress for each case is similar to that of the flap made with aluminum. This is because the overall geometry does not change significantly and, therefore, there are no new stress concentrators or abrupt section changes. Figure 18 shows the maximum

TABLE VII
FINITE-ELEMENT STATIC ANALYSIS CARRIED OUT OVER THE FLAP MADE WITH COMPOSITE MATERIAL.

Model Parameters	
Active Bodies	13
Number of Nodes	292070
Number of Elements	186266
Stiffness Behavior	Flexible
Max Structural Error	3.145
Min Structural Error	4.823E-02

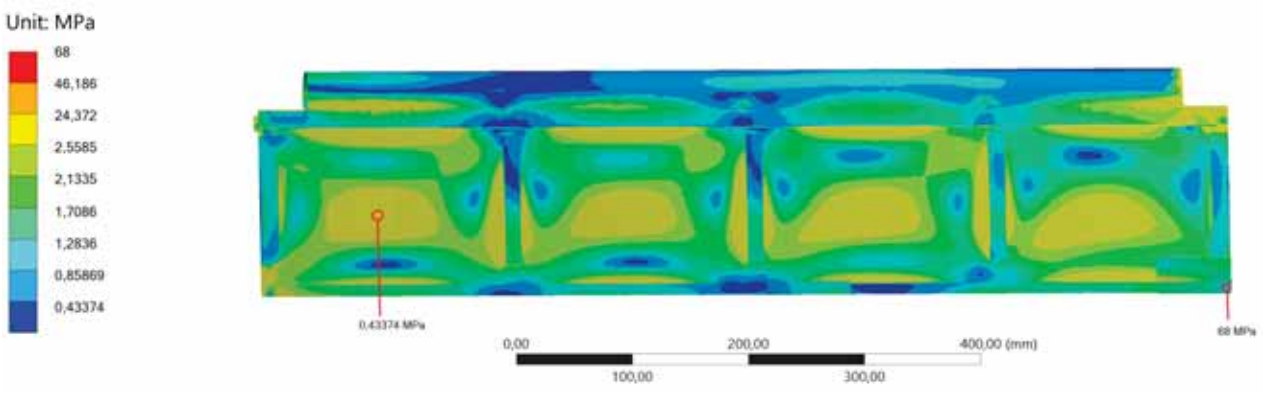

Fig. 13. Stress field of the flap made with aluminum.

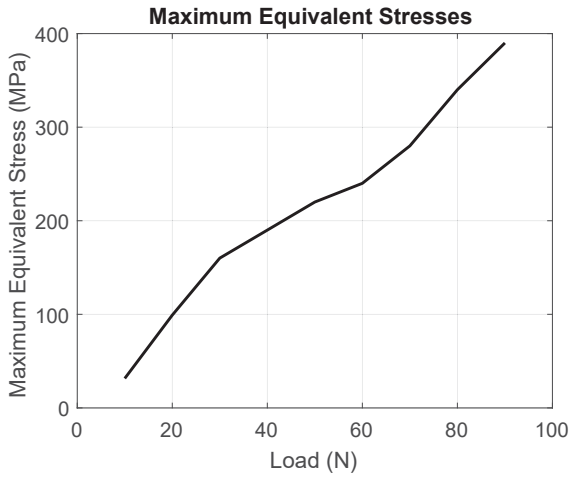

Fig. 14. Maximum stress of the flap made with aluminum.

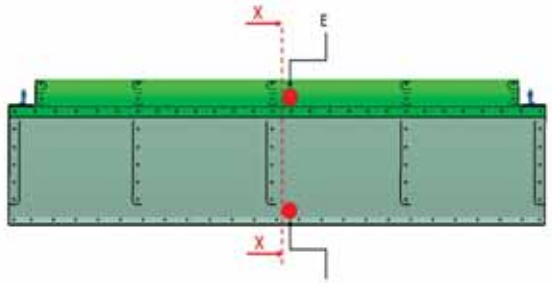

Fig. 15. Location of the point of interest.

stress over the flap made with composite materials. The deformation with respect to the vertical axis in the flap made with composite materials shows a greater deformation when compared with the one made with aluminum. The maximum vertical displacement measured is $0.70(\mathrm{mm})$ and the maximum calculated is $8.2(\mathrm{mm})$. The largest difference between the values experimentally measured and numerically calculated in the simulation is $0.21(\mathrm{mm})$, while the average error found is 24%. Figure 19 shows the deformation when each load condition applied. Table VIII shows the error values for each external load.

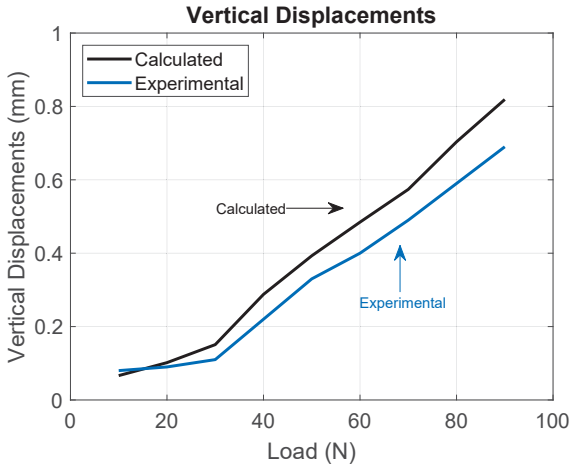

Fig. 16. Vertical displacement at the point of interest of the flap.

TABLE VIII
ESTIMATED ERROR FOUND FOR THE FLAP MADE WITH COMPOSITE MATERIAL.

Estimated Error					
Error	18.92	21.27	29.11	26.60	27.00
Step	1	2	3	4	5
Error	22.86	16.80	19.73	20.88	22.57
Step	6	7	8	9	**Avg.**

D. Discussion

In this subsection, general comments on the quality of the numerical results are reported and a brief discussion on the numerical analysis is provided.

1) Numerical Results of the Bulkhead Redesign: The main objective of the redesign and structural optimization is reducing the weight of the aircraft components of interest. This goal is achieved in this work. The component with the 6 plies of prepreg can reach weighing about $5.034(\mathrm{kg})$, which generates a weight decrease of approximately 44.16% when compared with the original design solution. However, this reduction in weight can be further optimized due to the low safety factor obtained with the failure criterion used. In future investigations, the Tsai-Wu constants will be calculated and the evaluation of this criterion could eliminate the level of uncertainty present in the current study.

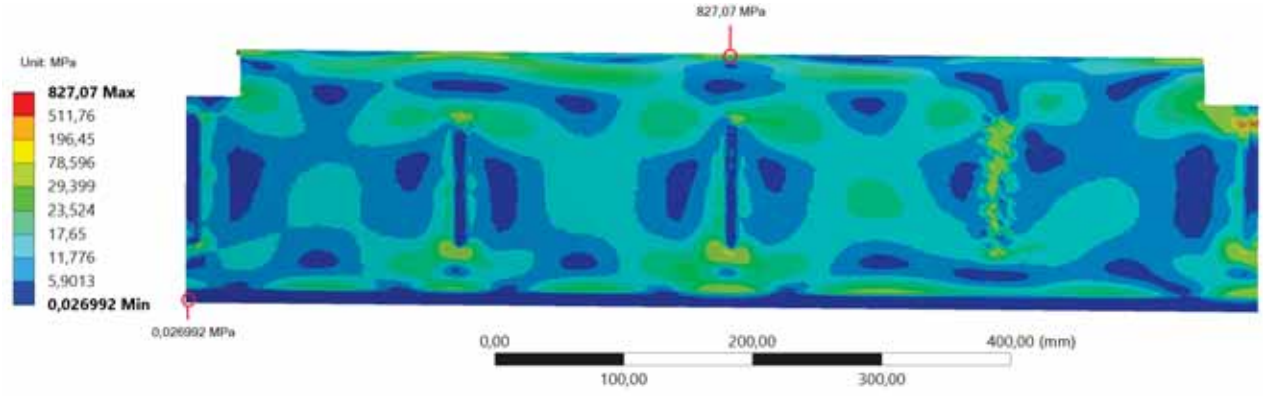

Fig. 17. Stress field of the flap made with composite materials.

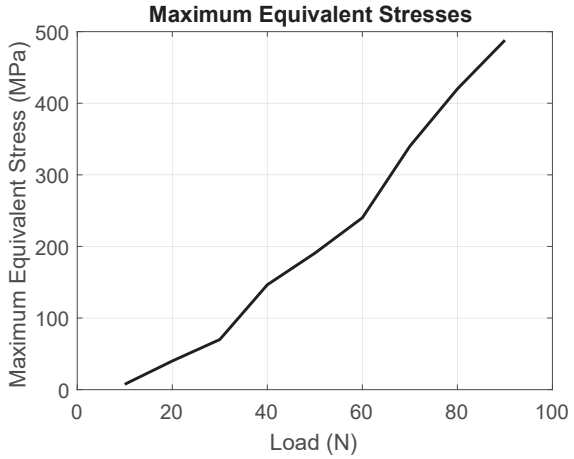

Fig. 18. Maximum stresses of the flap made with composite materials.

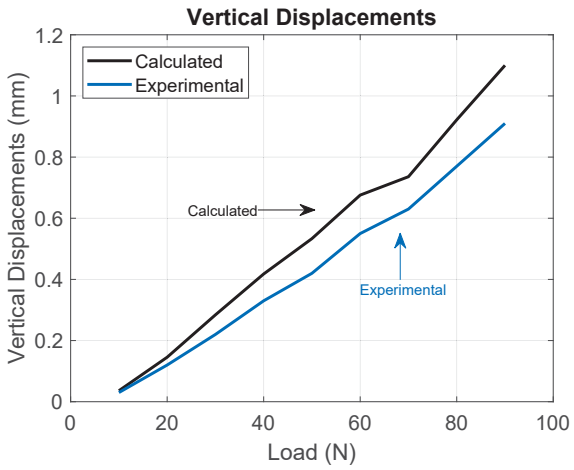

Fig. 19. Vertical displacement of the point of interest of the flap made with composite materials.

2) Comparison between the Two Flap Designs: The flap made with composite materials has a considerable increase in the vertical displacement as confirmed by experimental measurements. In the highest load condition, the difference is 31% with respect to the flap made of aluminum. However, this vertical displacement is still within the admissible limits. The final reduction in the weight, which is the principal objective of the redesign, is 18% and this structural optimization allows for obtaining the desired performance for the aircraft. However, as expected, the manufacturing costs increase accordingly. In future investigations, the optimization of the weight will be performed in a structural redesign process that takes also into account the cost of the material and the constraints in the budget for the redesign.

In Figure 20, the stress-strain curves of the flap made with aluminum and composites materials are represented. Observing Figure 20, it is apparent that composites materials offer the possibility of significantly bending the structures without snapping. However, the analysis presented in this work was carried within the elastic limit. Furthermore, the loads used for both types of elements are low. Therefore, although the flap made with composite materials has equivalent strain values slightly smaller due to the stiffness of the carbon fiber, the curve strain-stress of both materials is very similar, thereby confirming the physical significance of the numerical results found in this investigation.

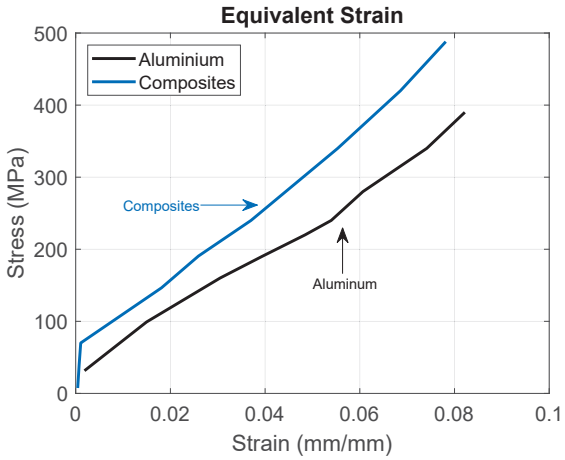

Fig. 20. Equivalent strains of the flap made with aluminum and with composite materials.

V. Summary, Conclusions, and Future Directions of Research

In general, the research of the authors is concerned with three main areas of interest pertaining to mechanical engineering, namely multibody dynamics, nonlinear control, and system identification. Multibody dynamics is focused on the study of the dynamic behavior of mechanical systems that comprise rigid and flexible bodies which are constrained by kinematic joints [89]–[92]. Nonlinear control is focused on the development of effective control strategies suitable for controlling mechanical systems described by nonlinear mathematical models [93]–[96]. System identification is focused on the determination of appropriate estimations of the parameters that serve to implement a dynamical model of a mechanical system [97]–[100]. This paper, on the other hand, deals with the redesign and optimization of the principal mechanical components that form the structural parts of an aircraft.

This research study presents the redesign of two important components of a general-aviation single-engine aircraft, namely the bulkhead and flap structural components. The performance of these components is evaluated by means of numerical analysis based on the finite element method and using experimental verifications. A simple optimization algorithm is also used for carrying out the structural redesign of the mechanical components considered in this paper. The flaps, originally made of aluminum, are redesigned using composites materials, thereby reducing the weight of the entire aircraft. In the redesign of the bulkhead, on the other hand, the use of pre-impregnated fiber carbon is studied. The redesign and the structural optimization of each mechanical component are evaluated through a finite element numerical analysis and by using a numerical optimization procedure. To this end, finite element models are developed and implemented in a virtual environment since the static analysis performed by using the finite element method represents an appropriate numerical technique suitable for addressing and solving the complex problem of interest for this investigation. In the finite element analysis performed in this investigation, the critical points of the structural components were identified and analyzed with several failure criteria in order to assess the viability of the material selection considered in the redesign phase. Furthermore, the quality of the numerical results obtained from the computational analysis developed in this work is assessed by using a set of experimental data available from an industrial partnership project involving the authors and local companies that manufacture aircraft components.

In this research work, the static performance of three fundamental aeronautical components is analyzed using a finite element approach. The mechanical components considered in this study are the bulkhead and two types of flaps. As demonstrated in this study, these mechanical components are capable of fully supporting the loading conditions imposed on the class of aircraft considered in this study. In particular, the bulkhead represents the principal structural component of a general-aviation single-engine which is used for supporting the weight of the engine and the external loads coming from the landing gear. The flaps, on the other hand, are commonly used for increasing the lift of the aircraft wings at a given airspeed. The bulkhead considered in this study is formed by a stack of prepreg carbon fibers. Two types of flaps are considered in this paper. The first type of flap is made of aluminum, while the second type of flap is composed of carbon fibers. In the static analysis of the flaps, these mechanical components are tested employing a set of loading conditions established by using aeronautical correlations. For this purpose, only a set of vertical forces is assumed as the externally applied loads, whereas fixed and pinned conditions due to the presence of bearings are employed as the boundary conditions. The set of applied forces and boundary conditions mentioned before are implemented in finite element models developed by the authors using the commercial software ANSYS and starting from CAD models of the mechanical components considered in this work. The CAD models employed in this investigation are highly detailed since these models were previously developed in the context of an industrial partnership agreement signed by the authors in collaboration with local companies that develop and manufacture aircraft structural components. Thus, the main contribution of the finite element analysis performed in this research work is the assessment of the reliability and the evaluation of the performance of the structural redesign carried out for the bulkhead and the flap components of a general-aviation single-engine aircraft.

Future research works will be devoted to the important topic of the Integration between the Computer-Aided Design and Analysis (I-CAD-A). Next-generation computer programs will allow for performing the geometric design, the simulation of the rigid body motion including large displacements and finite rotations, and the static and dynamic analysis of the structural components in a seamless environment, thereby enabling the engineers to obtain a robust design of a machine component that is optimal according to multiple criteria. The development of this new class of software requires the use of appropriate analytical techniques and advanced computational procedures, such as for example the Absolute Nodal Coordinate Formulation (ANCF) and the Isogeometric Analysis (IA), that will be the object of future investigations.

Author Contributions

This research paper was principally developed by the first author (Sergio Andrés Ardila-Parra). In the development of the paper, great support and guide were provided by the second author (Carmine Maria Pappalardo). The detailed review carried out by the third author (Octavio Andrés González Estrada) and by the fourth author (Domenico Guida) considerably improved the quality of the work.

References

[1] M. A. Jami'in and E. Julianto, "Hierarchical Algorithms of Quasi-Linear ARX Neural Networks for Identification of Nonlinear Systems," *Engineering Letters*, vol. 25, no. 3, pp321-328, 2017.

[2] J. Zhang, L. Yu, and L. Ding, "Velocity Feedback Control of Swing Phase for 2-DoF Robotic Leg Driven by Electro-hydraulic Servo System," *Engineering Letters*, vol. 24, no. 4, pp378-383, 2016.

[3] Q. W. Guo, W. D. Song, M. Gao, and D. Fang, "Advanced Guidance Law Design for Trajectory-Corrected Rockets with Canards under Single Channel Control," *Engineering Letters*, vol. 24, no. 4, pp469-477, 2016.

[4] H. Liu and Y. Li, "Safety Evaluation of a Long-Span Steel Trestle with an Extended Service Term Age in a Coastal Port Based on Identification of Modal Parameters," *Engineering Letters*, vol. 24, no. 1, pp84-92, 2016.

[5] I. I. Lazaro, A. Alvarez, and J. Anzurez, "The Identification Problem Applied to Periodic Systems Using Hartley Series," *Engineering Letters*, vol. 21, no. 1, pp36-43, 2013.

[6] F. Villecco and A. Pellegrino, "Evaluation of Uncertainties in the Design Process of Complex Mechanical Systems," *Entropy*, vol. 19, no. 9, 475, 2017.

[7] F. Villecco and A. Pellegrino, "Entropic Measure of Epistemic Uncertainties in Multibody System Models by Axiomatic Design," *Entropy*, vol. 19, no. 7, 291, 2017.

[8] R. Barbagallo, G. Sequenzia, A. Cammarata, S. M. Oliveri, and G. Fatuzzo, "Redesign and multibody simulation of a motorcycle rear suspension with eccentric mechanism," *International Journal on Interactive Design and Manufacturing (IJIDeM)*, vol. 12, no. 2, pp517-524, 2018.

[9] R. Barbagallo, G. Sequenzia, S. M. Oliveri, and A. Cammarata, "Dynamics of a high-performance motorcycle by an advanced multibody/control co-simulation," *Proceedings of the Institution of Mechanical Engineers, Part K: Journal of Multi-body Dynamics*, vol. 230, no. 2, pp207-221, 2016.

[10] A. Cammarata, "Unified formulation for the stiffness analysis of spatial mechanisms," *Mechanism and Machine Theory*, 105, pp272-284, 2016.

[11] A. Cammarata, "Optimized design of a large-workspace 2-DOF parallel robot for solar tracking systems," *Mechanism and Machine Theory*, 83, pp175-186, 2015.

[12] M. Culbreth, Y. Allaneau, and A. Jameson, "High-fidelity optimization of flapping airfoils and wings," In: Proceedings of the 29th AIAA Applied Aerodynamics Conference, pp3521, 2011.

[13] R. Citarella and G. Cricrí, "Three-dimensional BEM and FEM submodelling in a cracked FML full scale aeronautic panel," *Applied Composite Materials*, vol. 21, no. 3, pp557-577, 2014.

[14] R. Citarella, L. Federico, and A. Cicatiello, "Modal acoustic transfer vector approach in a FEM–BEM vibro-acoustic analysis," *Engineering Analysis with Boundary Elements*, vol. 31, no. 3, pp248-258, 2007.

[15] E. Onate, Structural analysis with the finite element method. Linear statics: Volume 1: Basis and solids, Springer Science and Business Media, 2013.

[16] E. Onate, Structural analysis with the finite element method. Linear statics: Volume 2: Beams, plates, and shells, Springer Science and Business Media, 2013.

[17] J. T. Katsikadelis, The Boundary Element Method for Engineers and Scientists: Theory and Applications, Academic Press, 2016.

[18] K. V. N. Gopal, "Product design for advanced composite materials in aerospace engineering," In: Advanced Composite Materials for Aerospace Engineering, Elsevier, pp413-428, 2016.

[19] H. T. Helali and M. Grafinger, "The precision of FEM simulation results compared with theoretical composite layup calculation," *Composites Part B: Engineering*, 95, pp282-292, 2016.

[20] G. Brown, "The use of composites in aircraft construction," http://vandaair.com/2014/04/14/the-use-of-composites-in-aircraft-construction, 2014.

[21] S. Rana and R. Fangueiro, Advanced composite materials for aerospace engineering: processing, properties and applications, Woodhead Publishing, 2016.

[22] E. C. Botelho, R. A. Silva, L. C. Pardini, and M. C. Rezende, "A review on the development and properties of continuous fiber/epoxy/aluminum hybrid composites for aircraft structures," *Materials Research*, vol. 9, no. 3, pp247-256, 2006.

[23] C. R. Bryant, D. A. McAdams, R. B. Stone, T. Kurtoglu, and M. I. Campbell, "A computational technique for concept generation," In: Proceedings of the ASME (American Society of Mechanical Engineers) 2005 International Design Engineering Technical Conferences and Computers and Information in Engineering Conference, pp267-276, 2005.

[24] J. Allison, D. Backman, and L. Christodoulou, "Integrated computational materials engineering: a new paradigm for the global materials profession," *Jom*, vol. 58, no. 11, pp25-27, 2006.

[25] D. Russo, C. Rizzi, "Structural optimization strategies to design green products," *Computers in industry*, vol. 65, no. 3, pp470-479, 2014.

[26] C. Soutis, "Carbon fiber reinforced plastics in aircraft construction," *Materials Science and Engineering: A*, vol. 412, no. 1-2, pp171-176, 2005.

[27] R. D. Buehrle, G. A. Fleming, R. S. Pappa, and F. W. Grosveld, "Finite element model development for aircraft fuselage structures," 2000.

[28] V. Mukhopadhyay, "Structural concepts study of non-circular fuselage configurations," 1996.

[29] E. A. Calado, M. Leite, and A. Silva, "Selecting composite materials considering cost and environmental impact in the early phases of aircraft structure design," *Journal of Cleaner Production*, 186, pp113-122, 2018.

[30] C. Kassapoglou, "Minimum cost and weight design of fuselage frames: Part A: design constraints and manufacturing process characteristics," *Composites Part A: Applied Science and Manufacturing*, vol. 30, no. 7, pp887-894, 1999.

[31] C. Kassapoglou, 'Minimum cost and weight design of fuselage frames: Part B: cost considerations, optimization, and results," *Composites Part A: Applied Science and Manufacturing*, vol. 30, no. 7, pp895-904, 1999.

[32] S. D. Thoppul, J. Finegan, and R. F. Gibson, "Mechanics of mechanically fastened joints in polymer - Matrix composite structures - A review," *Composites Science and Technology*, vol. 69, no. 3-4, pp301-329, 2009.

[33] R. Kaye and M. Heller, "Investigation of shape optimization for the design of life extension options for an F/A-18 airframe FS 470 bulkhead," *The Journal of Strain Analysis for Engineering Design*, vol. 35, no. 6, pp493-505, 2000.

[34] T. D. Marusich, S. Usui, and K. J. Marusich, "Finite element modeling of part distortion," In: International Conference on Intelligent Robotics and Applications, Springer, Berlin, Heidelberg, pp329-338, 2008.

[35] A. Germaneau, F. Peyruseigt, S. Mistou, P. Doumalin, and J. C. Dupre, "3D mechanical analysis of aeronautical plain bearings: Validation of a finite element model from measurement of displacement fields by digital volume correlation and optical scanning tomography," *Optics and Lasers in Engineering*, vol. 48, no. 6, pp676-683, 2010.

[36] M. Guida, F. Marulo, "Partial modeling of aircraft fuselage during an emergency crash landing," *Procedia Engineering*, 88, pp26-33, 2014.

[37] E. L. Fasanella and K. E. Jackson, "Crash simulation of a vertical drop test of a B737 fuselage section with auxiliary fuel tank," 2001.

[38] K. E. Jackson and E. L. Fasanella, "Crash simulation of a vertical drop test of a B737 fuselage section with overhead bins and luggage," In: Proceedings of the Third Triennial Aircraft Fire and Cabin Safety Conference, Atlantic City, NJ, pp22-25, 2001.

[39] I. Kumakura, M. Minegishi, K. Iwasaki, H. Shoji, N. Yoshimoto, H. Terada, T. Hayashi, "Vertical drop test of a transport fuselage section," SAE Technical Paper, No. 2002-01-2997, 2002.

[40] A. Ghali, A. Neville, and T. G. Brown, Structural Analysis: A Unified Classical and Matrix Approach, Crc Press, 2014.

[41] R. E. Melchers and A. T. Beck, Structural reliability analysis and prediction, John Wiley and Sons, 2018.

[42] L. U. Hansen, W. Heinze, and P. Horst, "Blended wing body structures in multidisciplinary pre-design," *Structural and Multidisciplinary Optimization*, vol. 36, no. 1, pp93-106, 2008.

[43] I. V. Ivanov, "Analysis, modelling, and optimization of laminated glasses as plane beam," *International Journal of Solids and Structures*, vol. 43, no. 22-23, pp6887-6907, 2006.

[44] A. Esnaola, B. Elguezabal, J. Aurrekoetxea, I. Gallego, and I. Ulacia, "Optimization of the semi-hexagonal geometry of a composite crush structure by finite element analysis," *Composites Part B: Engineering*, 93, pp56-66, 2016.

[45] J. Sliseris, G. Frolovs, K. Rocens, and V. Goremikins, "Optimal design of GFRP-plywood variable stiffness plate," *Procedia Engineering*, 57, pp1060-1069, 2013.

[46] V. Mukhopadhyay, J. Sobieszczanski-Sobieski, I. Kosaka, G. Quinn, and G. N. Vanderpaats, "Analysis, design, and optimization of noncylindrical fuselage for blended-wing-body vehicle," *Journal of Aircraft*, vol. 41, no. 4, pp925-930, 2004.

[47] R. A. Witik, F. Gaille, R. Teuscher, H. Ringwald, V. Michaud, and J. A. E. Manson, "Economic and environmental assessment of alternative production methods for composite aircraft components," *Journal of Cleaner Production*, 29, pp91-102, 2012.

[48] K. T. Van Den Kieboom, and A. Elham, "Concurrent wing and high-lift system aerostructural optimization," *Structural and Multidisciplinary Optimization*, vol. 57, no. 3, pp947-963, 2018.

[49] J. K. S. Dillinger, T. Klimmek, M. M. Abdalla, and Z. Gurdal, "Stiffness optimization of composite wings with aeroelastic constraints," *Journal of Aircraft*, vol. 50, no. 4, pp1159-1168, 2013.

[50] O. T. Thomsen and J. R. Vinson, "Analysis and parametric study of non-circular pressurized sandwich fuselage cross section using a high-order sandwich theory formulation," *Journal of Sandwich Structures and Materials*, vol. 3, no. 3, pp220-250, 2001.

[51] D. Liu, H. Lohse-Busch, V. Toropov, C. Huhne, and U. Armani, "Detailed design of a lattice composite fuselage structure by a mixed

optimization method," *Engineering Optimization*, vol. 48, no. 10, pp1707-1720, 2016.
[52] L. Krog, A. Tucker, M. Kemp, and R. Boyd, "Topology optimisation of aircraft wing box ribs," In: Proceeding of the 10th AIAA/ISSMO multidisciplinary analysis and optimization conference, p. 4481, 2004.
[53] R. Arravind, M. Saravanan, R. M. Rijuvan, and D. Vadivel, "Design, analysis and simulation of a composite bulkhead," In: Proceedings of the International Conference on Mechanical and Industrial Engineering (ICMIE'12) on 16-12-2012, Nagpur, 2005.
[54] T. Wang and J. Maxon, "Application of statistical energy analysis and optimization in the design of Gulfstream large-cabin aircraft interior thermal/acoustic package," In: Proceedings of the INTER-NOISE and NOISE-CON congress and conference proceedings, Institute of Noise Control Engineering, vol. 2008, no. 7, pp2073-2084, 2008.
[55] S. Ding and X. Zhou, "Structural design and optimization of a morphing wing trailing edge flap," *Aerospace Systems*, vol. 1, no. 2, pp109-119, 2018.
[56] R. Kienzler and G. Herrmann, "Mechanics in material space: with applications to defect and fracture mechanics," Springer Science and Business Media, vol. 11, 2012.
[57] R. T. Haftka and Z. Gurdal, "Elements of structural optimization," Springer Science and Business Media, vol. 11, 2012.
[58] N. V. Queipo, R. T. Haftka, W. Shyy, T. Goel, R. Vaidyanathan, and P. K. Tucker, "Surrogate-based analysis and optimization," *Progress in aerospace sciences*, vol. 41, no. 1, pp.1-28, 2005.
[59] R. T. Haftka and R. V. Grandhi, "Structural shape optimization - A survey," *Computer methods in applied mechanics and engineering*, vol. 57, no. 1, pp91-106, 1986.
[60] R. T. Haftka and B. Prasad, "Optimum structural design with plate bending elements-a survey," *AIAA Journal*, vol. 19, no. 4, pp517-522, 1981.
[61] S. Venkataraman and R. Haftka, "Structural Optimization: What has Moore's Law done for us?," In: 43rd AIAA/ASME/ASCE/AHS/ASC Structures, Structural Dynamics, and Materials Conference, p. 1342, 2002.
[62] G. J. Kennedy and J. R. Martins, "A parallel finite-element framework for large-scale gradient-based design optimization of high-performance structures," *Finite Elements in Analysis and Design*, 87, pp56-73, 2014.
[63] R. P. Henderson, J. R. Martins, and R. E. Perez, "Aircraft conceptual design for optimal environmental performance," *The Aeronautical Journal*, vol. 116, no. 1175, pp1-22, 2012.
[64] C. M. Pappalardo, M. C. De Simone, and D. Guida, "Multibody modeling and nonlinear control of the pantograph/catenary system," *Archive of Applied Mechanics*, vol. 89, no. 8, pp1589-1626, 2019.
[65] J. R. Martins, J. J. Alonso, and J. J. Reuther, "A coupled-adjoint sensitivity analysis method for high-fidelity aero-structural design," *Optimization and Engineering*, vol. 6, no. 1, pp33-62, 2005.
[66] A. A. Shabana, Computational Continuum Mechanics, John Wiley and Sons, 2018.
[67] C. M. Pappalardo, T. Wang, and A. A. Shabana, "On the formulation of the planar ANCF triangular finite elements," *Nonlinear Dynamics*, vol. 89, no. 2, pp1019-1045, 2017.
[68] C. M. Pappalardo, T. Wang, and A. A. Shabana, "Development of ANCF tetrahedral finite elements for the nonlinear dynamics of flexible structures," *Nonlinear Dynamics*, vol. 89, no. 4, pp2905-2932, 2017.
[69] C. M. Pappalardo, Z. Zhang, and A. A. Shabana, "Use of independent volume parameters in the development of new large displacement ANCF triangular plate/shell elements," *Nonlinear Dynamics*, vol. 91, no. 4, pp2171-2202, 2018.
[70] K. J. Bathe, Finite Element Procedures, Prentice Hall, 2006.
[71] T. J. Hughes, The finite element method: Linear static and dynamic finite element analysis, Courier Corporation, 2012.
[72] O. C. Zienkiewicz, R. L. Taylor, and R. L. Taylor, The finite element method: Solid mechanics, Volume 2, Butterworth-Heinemann, 2000.
[73] J. Bonet and R. D. Wood, Nonlinear continuum mechanics for finite element analysis, Cambridge university press, 1997.
[74] A. A. Shabana, Dynamics of Multibody Systems, Cambridge University Press, 2013.
[75] T. Belytschko, W. K. Liu, B. Moran, and K. Elkhodary, Nonlinear finite elements for continua and structures, John wiley and Sons, 2013.
[76] C. M. Pappalardo, "A natural absolute coordinate formulation for the kinematic and dynamic analysis of rigid multibody systems," *Nonlinear Dynamics*, vol. 81, no. 4, pp1841-1869, 2015.
[77] A. A. Shabana, Computational Dynamics, John Wiley and Sons, 2009.
[78] P. Sirisalee, G. T. Parks, P. J. Clarkson, and M. F. Ashby, "A new approach to multi-criteria material selection in engineering design," In: DS 31, Proceedings of ICED 03, the 14th International Conference on Engineering Design, Stockholm, pp451-452, 2003.
[79] R. L. Keeney and H. Raiffa, Decisions with Multiple Objectives: Preferences and Value Trade-Offs, Cambridge University Press, 1993.
[80] M. F. Ashby, "Multi-objective optimization in material design and selection," *Acta materialia*, vol. 48, no. 1, pp359-369, 2000.
[81] P. E. Illman and G. E. Gailey, The pilot's handbook of aeronautical knowledge, McGraw-Hill, 2000.
[82] E. J. Barbero, Finite element analysis of composite materials using ANSYS®, CRC press, 2013.
[83] H. Laith, H. Kareem, N. Natik, ANSYS Workbench for mechanical engineering: A step by step to learn ANSYS Workbench, 2015.
[84] M. R. Hatch, Vibration simulation using MATLAB and ANSYS, Chapman and Hall-CRC, 2000.
[85] H. H. Lee, Finite Element Simulations with ANSYS Workbench 18, SDC Publications, 2018.
[86] T. Stolarski, Y. Nakasone, S. Yoshimoto, Engineering analysis with ANSYS software, Butterworth-Heinemann, 2018.
[87] M. J. Hinton, A. S. Kaddour, and P. D. Soden, Failure criteria in fibre reinforced polymer composites: the world-wide failure exercise, Elsevier, 2004.
[88] R. M. Jones, Mechanics of composite materials, CRC press, 2018.
[89] M. C. De Simone, S. Russo, Z. B. Rivera, and D. Guida, "Multibody Model of a UAV in Presence of Wind Fields," Proceedings - 2017 International Conference on Control, Artificial Intelligence, Robotics and Optimization, ICCAIRO 2017, 2018-January, pp83-88, 2018.
[90] M. C. De Simone, Z. B. Rivera, and D. Guida, "A New Semi-Active Suspension System for Racing Vehicles," *FME Transactions*, vol. 45, no. 4, pp579, 2017.
[91] M. C. De Simone and D. Guida, "On the Development of a Low Cost Device for Retrofitting Tracked Vehicles for Autonomous Navigation," Proceedings of the XXIII Conference of the Italian Association of Theoretical and Applied Mechanics (AIMETA 2017), 4-7 Spetember 2017, Salerno, Italy, 2017.
[92] A. Ruggiero, M. C. De Simone, D. Russo, and D. Guida, "Sound pressure measurement of orchestral instruments in the concert hall of a public school," *International Journal of Circuits, Systems and Signal Processing*, 10, pp75-812, 2016.
[93] M. C. De Simone and D. Guida, "Dry Friction Influence on Structure Dynamics," COMPDYN 2015 - 5th ECCOMAS Thematic Conference on Computational Methods in Structural Dynamics and Earthquake Engineering, pp4483-4491, 2015.
[94] A. Ruggiero, S. Affatato, M. Merola, and M. C. De Simone, "FEM analysis of metal on UHMWPE total hip prosthesis during normal walking cycle," Proceedings of the XXIII Conference of The Italian Association of Theoretical and Applied Mechanics (AIMETA 2017), Salerno, Italy; 4-7 September 2017, (2017), 2017.
[95] M. C. De Simone, Z. B. Rivera, and D. Guida, "Obstacle Avoidance System for Unmanned Ground Vehicles by using Ultrasonic Sensors," *Machines*, vol. 6, no. 2, 18, 2018.
[96] V. Iannone and M. C. De Simone, "Modelling of a DC Gear Motor for Feed-Forward Control Law Design for Unmanned Ground Vehicles," Actuators, In press, 2018.
[97] A. Quatrano, M. C. De Simone, Z. B. Rivera, and D. Guida, "Development and Implementation of a Control System for a Retrofitted CNC Machine by Using Arduino," *FME Transactions*, vol. 45, pp578-584, 2017.
[98] M. C. De Simone and D. Guida, "Modal Coupling in Presence of Dry Friction," *Machines*, vol. 6, no.1, 8, 2018.
[99] M. C. De Simone and D. Guida, "Identification and control of a Unmanned Ground Vehicle by using Arduino," *UPB Scientific Bulletin, Series D: Mechanical Engineering*, vol. 80, no. 1, pp141-154, 2018.
[100] M. C. De Simone, Z. B. Rivera, and D. Guida, "Finite Element Analysis on Squeal-Noise in Railway Applications," *FME Transactions*, vol. 46, no. 1, pp93-100, 2018.